Journal of Human Evolution 57 (2009) 608–622

Contents lists available at ScienceDirect

Journal of Human Evolution

journal homepage: www.elsevier.com/locate/jhevol

Size, shape, and asymmetry in fossil hominins: the status of the LB1 cranium based on 3D morphometric analyses

Karen L. Baab [a,*], Kieran P. McNulty [b]

[a] Department of Anatomical Sciences, Stony Brook University Medical Center, Stony Brook, NY 11794, USA
[b] Department of Anthropology, University of Minnesota, 395 Hubert H., Humphrey Center, 301 19th Avenue S, Minneapolis, MN 55455, USA

ARTICLE INFO

Article history:
Received 18 January 2008
Accepted 23 July 2008

Keywords:
Liang Bua
Homo floresiensis
Static allometry
Asymmetry
Geometric morphometrics

ABSTRACT

The unique set of morphological characteristics of the Liang Bua hominins (*Homo floresiensis*) has been attributed to explanations as diverse as insular dwarfism and pathological microcephaly. This study examined the relationship between cranial size and shape across a range of hominin and African ape species to test whether or not cranial morphology of LB1 is consistent with the basic pattern of static allometry present in these various taxa. Correlations between size and 3D cranial shape were explored using principal components analysis in shape space and in Procrustes form space. Additionally, patterns of static allometry within both modern humans and Plio-Pleistocene hominins were used to simulate the expected cranial shapes of each group at the size of LB1. These hypothetical specimens were compared to LB1 both visually and statistically. Results of most analyses indicated that LB1 best fits predictions for a small specimen of fossil *Homo* but not for a small modern human. This was especially true for analyses of neurocranial landmarks. Results from the whole cranium were less clear about the specific affinities of LB1, but, importantly, demonstrated that aspects of facial morphology associated with smaller size converge on modern human morphology. This suggests that facial similarities between LB1 and anatomically modern humans may not be indicative of a close relationship. Landmark data collected from this study were also used to test the degree of cranial asymmetry in LB1. These comparisons indicated that the cranium is fairly asymmetrical, but within the range of asymmetry exhibited by modern humans and all extant African ape species. Compared to other fossil specimens, the degree of asymmetry in LB1 is moderate and readily explained by the taphonomic processes to which all fossils are subject. Taken together, these findings suggest that *H. floresiensis* was most likely the diminutive descendant of a species of archaic *Homo*, although the details of this evolutionary history remain obscure.

Introduction

Much of the debate surrounding interpretation of the Liang Bua hominins has thus far focused on the single cranium recovered in excavation, Liang Bua 1 (LB1). Like other specimens found in the karst cave of Liang Bua on the Indonesian island of Flores, this individual was small in stature, likely standing at just over one meter in height (Brown et al., 2004; see also Morwood et al., 2004). A mix of primitive, derived, and unique features found in the these hominins, in combination with the small size of the LB1 brain, has inspired a great deal of subsequent research and commentary about the affinities of this fossil (e.g., Henneberg and Thorne, 2004; Morwood et al., 2005; Falk et al., 2005, 2006, 2007; Weber et al., 2005; Argue et al., 2006; Jacob et al., 2006; Martin et al., 2006a,b; Richards, 2006). Several previous analyses suggest that LB1 most closely resembles *Homo erectus sensu lato* in both generalized and more detailed aspects of the cranium and endocast (Brown et al., 2004; Falk et al., 2005, 2007; Gordon et al., 2008). However, its very small endocranial capacity of 417 cm^3 (Falk et al., 2005) is outside of the recorded range for this species, even if one includes the smaller fossils from Africa and Dmanisi. Moreover, numerous features of the postcranial skeleton in Liang Bua specimens seem more suggestive of australopiths than they do of the KNM-WT 15000 *H. erectus* skeleton (Brown et al., 2004; Morwood et al., 2005; Tocheri et al., 2007).

The small relative brain size of LB1, even when taking into account the stature of this individual, has prompted an alternative hypothesis that LB1 was a modern human with microcephaly rather than the type specimen of a new species (Henneberg and Thorne, 2004; Jacob et al., 2006). In support of this, Jacob et al. (2006; see also Richards, 2006) observed that, individually, many of

* Corresponding author.
E-mail addresses: Karen.Baab@sunysb.edu (K.L. Baab), kmcnulty@umn.edu (K.P. McNulty).

0047-2484/$ – see front matter © 2008 Elsevier Ltd. All rights reserved.
doi:10.1016/j.jhevol.2008.08.011

the cranial and mandibular traits fall within the modern human range, with several features frequently present in Australomelanesian populations. Pathologically high levels of cranial asymmetry in LB1 were also cited as evidence that this individual suffered from microcephaly. Articles supporting (Weber et al., 2005; Martin et al., 2006a, b) or denouncing (Falk et al., 2005, 2006, 2007; Argue et al., 2006) this diagnosis of microcephaly have since appeared in the literature and no consensus opinion has been reached. More recently, other researchers have diagnosed LB1 with endemic cretinism (Obendorf et al., 2008) or with Laron Syndrome (Hershkovitz et al., 2007; but see Falk et al., 2008).

The presence of at least twelve individuals from the Liang Bua cave (W. Jungers, pers. comm.) confirms that the short stature of LB1 was characteristic of the population rather than an individual pathology. Given this fact, the most conservative explanation for LB1's cranial morphology is that it reflects patterns of size-correlated shape variability observed in closely related groups. In other words, if the unique features of the Flores fossils can be expected solely from the established body sizes, then additional explanations for the morphology may not be required. And, while it is unlikely that the autapomorphic postcranial morphology can be predicted by models of static allometry, only recently have aspects of the external cranial morphology been examined in this regard (Baab et al., 2007; Nevell et al., 2007; Gordon et al., 2008).

Comparisons with observed patterns of static allometry cannot indict any causal mechanism (e.g., insular dwarfism) for the change in body size (Leigh et al., 2003), nor do they rule out other factors for explaining the morphology, should such evidence be discovered and verified. Rather, this approach is based on the testable hypothesis that the LB1 cranial morphology reflects patterns of size-correlated shape change observed in either extant or fossil human groups.

The morphology of the LB1 cranium

Brown et al. (2004) and Morwood et al. (2004, 2005) have described the remains of at least nine individuals attributed to *H. floresiensis*, as well as associated archaeological artifacts. And while the only known cranial specimen has a brain size and stature comparable to those of Pliocene australopiths, its craniodental morphology is most consistent with attribution to the genus *Homo* (Brown et al., 2004). In common with other members of this genus, LB1 has a shorter and more orthognathic face with smaller cheek teeth compared to the australopiths (Brown et al., 2004). The original description highlighted many features of the neurocranium that align LB1 with archaic *Homo* (fossil *Homo* specimens excluding anatomically modern *H. sapiens*) in general, and *H. erectus* (*s.l.*) in particular, such as the long, low cranial profile, sagittal angulation of the occipital bone, a mound-like occipital torus, presence of a mastoid fissure, and surprisingly thick cranial bones. The presence of these traits in *H. erectus s.l.* is well documented and helps to distinguish this taxon from *H. sapiens* (Weidenreich, 1943, 1951; Le Gros Clark, 1964; Howell, 1978; Howells, 1980; Rightmire, 1990; Antón, 2003). Although some traits may be primitive retentions from earlier hominins (e.g., Andrews, 1984), together they serve as components of a combination species definition for *H. erectus* (*sensu* Wood, 1984; Turner and Chamberlain, 1989; Rightmire, 1990; Baab, 2007). An alternative possibility is that LB1 bears stronger resemblances to earlier African *H. erectus* (= *H. ergaster*) than to Javanese *H. erectus* (Brown et al., 2004; Argue et al., 2006).

Hominin evolutionary history and biogeography in Southeast Asia

Geographic and temporal considerations suggest three possibilities for the ancestry of the Flores hominins. Modern humans are one such group, having already become well established in the region by the dates associated with the Liang Bua remains (Barker, 2002; Gillespie, 2002). Alternatively, *H. erectus* is also known from this area and dated to as late as ~100 ka (Bartstra et al., 1988) or 50-32 ka (Swisher et al., 1996) on the nearby island of Java. A third possibility is that the Liang Bua hominins were descended from a fossil human group currently unknown or unrecognized in this region (Brown et al., 2004; Argue et al., 2006).

H. erectus has been documented on the nearby island of Java throughout much of the Pleistocene (Swisher et al., 1994, 1996; Swisher, 1997; Larick et al., 2001), although the dates of both the first and last appearance of the species in this region have proven controversial (e.g., Swisher et al., 1994, 1996; Grün and Thorne, 1997; Huffman, 2001; Westaway et al., 2003; Dennell, 2005; Huffman et al., 2005, 2006). Hominins reached the Soa Basin (on Flores east of Liang Bua) as early as ~800-700 ka (Sondaar, 1984; Sondaar et al., 1994; Morwood et al., 1997, 1998, 1999; Brumm et al., 2006). An earlier date of 880 ka is possible (M. Morwood, pers. comm.), based on the presence of lithic artifacts. As the Soa Basin sites are not associated with hominin fossils, the maker of these tools can only be inferred from the timeframe to be *H. erectus*. Interestingly, Brumm et al. (2006) have argued for technological continuity between the Soa Basin and Liang Bua stone tools, despite a gap of nearly 600 k.yr. This argument contradicts suggestions (e.g., Lahr and Foley, 2004; Martin et al., 2006a) that the complexity of lithic artifacts from the same layers as *H. floresiensis* dictates their production by modern *H. sapiens*.

Jacob et al. (2006) argued that it is unlikely that *H. erectus* could have reached the island of Flores only once and remained isolated until the Holocene arrival of modern *H. sapiens*. Considering the dispersal barriers between Java and Flores, however, the scenario of a single hominin colonization event seems at least as plausible as a hypothesis of multiple dispersals. Numerous separate lines of evidence are consistent with relative isolation of Flores from both the Sunda Shelf to the west and Australia/New Guinea to the east. In general, the islands situated between the Sunda Shelf and the Sahul, sometimes referred to as Wallacea, exhibit high levels of terrestrial vertebrate endemicity (How et al., 1996; Kitchener and Suyanto, 1996; How and Kitchener, 1997), and Flores in particular was home to an impoverished island fauna (Sondaar, 1987; Cox, 2000; van den Bergh et al., 2001), which included dwarfed *Stegodon* (Azzaroli, 1981; Morwood et al., 2005) and giant rodents and tortoises (Davis, 1985; van den Bergh et al., 2001, 2009). This endemicity is likely due to the role that strong currents in the Lombok and Sape straits (between Bali and Lombok and between Sumbawa and Flores, respectively) played as dispersal barriers to terrestrial vertebrates (van den Bergh et al., 2001). Even at the last glacial maximum, when sea levels were as much as 115–125 m below present levels (Lambeck and Chappell, 2001), Bali and Lombok lacked a land connection (see Fig. 1 in Voris, 2000), implying no connection between Flores and the Sunda Shelf to the west. Various ecological and climatic variables related to the Lesser Sunda Islands (including Flores) may also have acted as barriers to dispersal of large mammals in the eastern Indonesian islands (Mayr, 1944; Brandon-Jones, 1998), as evidenced by the recovery of only a single large-bodied mammal, *Stegodon*, from pre-Holocene deposits on Flores.

While most discussion has focused on either modern humans or *H. erectus* as the likely source for the Liang Bua hominins, Brown et al. raised the third possibility that "an unknown small-bodied and small-brained hominin may have arrived on Flores from the Sunda Shelf" (2004: 1060). This viewpoint was supported by morphometric and comparative analyses of the Flores skeletal material (Morwood et al., 2005; Argue et al., 2006), which emphasized the uniquely mosaic nature of the LB1 anatomy. This hypothesis may imply that *H. floresiensis* was part of a more extensive lineage already characterized by small stature and brain size. The many primitive characteristics of *H. floresiensis*, particularly in the postcranial skeleton (Morwood et al., 2005; Tocheri

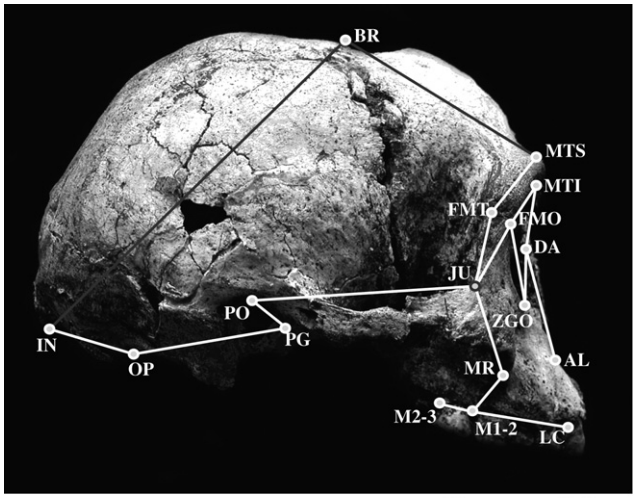

Photo courtesy P. Brown

Figure 1. The neurocranium + face landmark set illustrated on the LB1 cranium. The wireframe connecting landmarks is for visualization purposes and does not represent actual data. Landmark abbreviations and definitions can be found in Table 2. The OP and LCAN landmarks are not actually visible in this view but their approximate positions are indicated.

et al., 2007; Jungers et al., 2008), further suggest that this ancestor would be less derived than the African *H. erectus* skeleton KNM-WT 15000. In fact, the possibility has been raised that the initial hominins to migrate out of Africa were actually members of early *Homo* (e.g., *H. habilis*) rather than *H. erectus* (Robinson, 1953; Tobias and von Koenigswald, 1964; Krantz, 1975; Howell, 1978; Franzen, 1985; Clarke, 1990, 2000; Swisher et al., 1994; White, 1995; Wang and Tobias, 2001; Dennell and Roebroeks, 2005).

The site of Dmanisi, Georgia (de Lumley et al., 2006; Rightmire et al., 2006) and perhaps the Sangiran dome (Kaifu et al., 2005) may provide fossil evidence for a more primitive hominin dispersal out of Africa. Stature reconstruction for the Dmanisi hominins, based on postcranial evidence, is between 1.45 and 1.66 m (Lordkipanidze et al., 2007) — considerably shorter than the 1.85 m predicted for an adult KNM-WT 15000 (Ruff and Walker, 1993). Moreover, their endocranial volumes range from 612–775 cm^3 (Rightmire et al., 2006), well below the average for other *H. erectus* crania ($\sim$1100 cm^3) and even for specimens from East Turkana (804–848 cm^3). Kaifu et al. (2005) argued that the earliest, but least complete, specimens from the Sangiran Formation (>1.5 Ma; Larick et al., 2001) and lowest layers of the Bapang Formation ($\sim$1.5 Ma) share dental features with the Dmanisi hominins and are more primitive than even the East Turkana *H. erectus* sample.

All of these observations are consistent with the presence of a less-derived and possibly smaller form of hominin outside of Africa prior to the earliest appearance of *H. floresiensis* at 95–74 ka (Morwood et al., 2005). LB1 is still considerably smaller than even these specimens, however, suggesting that some degree of size reduction occurred within the Liang Bua lineage. The hypothesis that LB1's cranial morphology fits observed patterns of size correlated shape change does not require any specific mechanism of reduction. In that sense, whether the Liang Bua lineage became smaller in isolation on an island (Brown et al., 2004; Morwood et al., 2004), through ecological isolation like some modern human populations (Cavalli-Sforza, 1986; Shea and Bailey, 1996), or through some other process is irrelevant to the basic model of body size reduction. And, while static allometry certainly cannot account for all of the morphological differences between LB1 and other living and fossil hominins, it is necessary to first determine the features associated with size reduction before one can adequately evaluate alternative hypotheses.

In this project, we assessed the affinities of the LB1 cranium based on 3D cranial shape, with special attention to the relationship between cranial size and shape within extinct and extant hominin taxa. We used models of static allometry to examine whether or not the shape of the LB1 cranium is consistent with a small member of the genus *Homo*. In addition, we examined the second-order hypothesis of pathological microcephaly by measuring asymmetries in the LB1 cranium (e.g., Jacob et al., 2006). All analyses utilized 3D geometric morphometric methods to quantify and visualize shape differences.

Materials

To examine patterns of size-correlated shape change and assess the degree of cranial asymmetry, 3D landmark data were collected from a stereolithographic model of the LB1 cranium generated from a CT scan (described in Brown et al., 2004); dimensions of the model were verified by comparison to the measurements on the original specimen (P. Brown, personal communication). The same data were also acquired from a representative sample of fossil and extant hominins as well as from large comparative samples of African apes (Table 1). All data were collected from original fossil specimens with the exception of the Dmanisi and Zhoukoudian samples, Sangiran 17, Dali, La Chapelle aux Saints, and La Ferrassie 1, for which original fossils were not available. Samples of the modern taxa are approximately evenly distributed between males and females. Modern humans were sampled from 11 different geographic groups in Africa, Asia, Australia, Europe, and North America, including two groups of small-statured modern humans, the Andaman Islanders and the Khoe-San. African ape specimens were wild shot, and samples of *Pan troglodytes* and *Gorilla gorilla* included representatives from three subspecies each. All specimens were adults with the exception of KNM-WT 15000 and D2700, included here because they are among the few available *H. erectus* specimens that preserve both facial and neurocranial landmarks. While the age of Zhoukoudian 3 (Zkd 3) is unclear (cf. Black, 1929, 1931; Weidenreich, 1943; Mann, 1971; Antón, 2001), previous 3D analyses have indicated that Zkd 3 fits well within the range of cranial shape variation for adult Zhoukoudian specimens (Baab, in press).

The Zhoukoudian male reconstructed by Tattersall and Sawyer (1996) was also used here as there are no complete faces in the Zhoukoudian sample, and only one reasonably complete face is known for Asian *H. erectus* as a whole (Sangiran 17). The Zhoukoudian reconstruction is an amalgam of the neurocranium (including the supraorbital torus) of Zkd 12 and facial fragments from several other individuals. Zkd 12 is one of the larger specimens from the Zhoukoudian collection, and all facial fragments used in the reconstruction were also relatively large (Tattersall and Sawyer, 1996).

A series of 35 homologous landmarks provided the basic data for morphometric analysis (Table 2). Midline and bilateral landmarks (Table 2) representing the cranial vault, face, lateral temporal base, and supraorbital torus (see Frost et al., 2003; Harvati et al., 2004; McNulty et al., 2006; Baab, 2007) were recorded in three dimensions from each specimen with a Microscribe 3DX digitizer. Different subsets of these landmarks were used for each particular analysis (also indicated in Table 2), maximizing fossil sample sizes. Two subsets were used to examine the shape of the cranium: one that included both neurocranial and facial data, and one that only used neurocranial landmarks (illustrated in Figs. 1 and 2, respectively). "Neurocranial," in this respect, included ectocranial landmarks from both the cranial vault and base. Only a limited number of fossil hominin specimens ($n = 12$) were complete enough for inclusion in the neurocranium + face analysis. While the second landmark set excluded the facial skeleton, it used a denser sampling of landmarks from the neurocranium (the neurocranium-only

Table 1
Sample composition and taxonomic assignments of specimens in neurocranium + face and neurocranium-only data sets.

Analysis	Neurocranium + Face[a]	Neurocranium-Only[a]
H. floresiensis	$n = 1$ LB1	$n = 1$ LB1
Plio-Pleistocene *Homo*	$n = 8$ *H. habilis*: KNM-ER 1813 *H. erectus*: KNM-ER 3733, KNM-WT 15000, D2700, S 17, Zhoukoudian reconstruction mid-Pleistocene *Homo*: Kabwe, Petralona	$n = 20$ *H. habilis*: KNM-ER 1813 *H. erectus*: KNM-ER 3733, KNM-ER 3883, Daka, D2280, D3444, S 17, Sm 1, Sm 3, Ng 6, Ng 10, Ng 11, Ng 12, Zkd 11, Zkd 12 mid-Pleistocene *Homo*: Omo 2, Dali, Kabwe Neanderthals: La Chapelle aux Saints, La Ferrassie 1
Australopiths	$n = 4$ *A. africanus*: Sts 5, Sts 71 *P. boisei*: OH 5, KNM-ER 406	N/A
Modern *H. sapiens*	$n = 324$	$n = 395$ includes Skhul 5
P. paniscus	$n = 44$	N/A
P. troglodytes	$n = 117$ Includes *P.t. troglodytes*, *P.t. schweinfurthii*, *P.t. verus*	N/A
G. gorilla	$n = 95$ Includes *G.g. gorilla*, *G.g. beringei*, *G.g. graueri*	N/A

[a] Abbreviations are as follows: LB – Liang Bua, KNM-ER – Kenya National Museums-East Rudolf, KNM-WT – Kenya National Museums-West Turkana, D – Dmanisi, S – Sangiran, Sm – Sambungmacan, Ng – Ngandong, Zkd – Zhoukoudian, Sts – Sterkfontein, OH – Olduvai Hominid.

landmark set) and allowed for the inclusion of many more fossils ($n = 20$), particularly from *H. erectus*. Differences in landmark protocols excluded the extant ape samples from neurocranium-only analyses. Analyses of asymmetry incorporated some additional landmarks (see Table 2) and focused mainly on facial morphology (cf. Jacob et al., 2006).

Methods

Geometric morphometrics

We applied geometric morphometric methodologies to 3D landmark data in order to explore the affinities of LB1, the relationship between size and cranial shape, and the degree of asymmetry in extant and fossil specimens. We maximized sample sizes by reflecting antimeres of missing bilateral landmarks across the geometric midline plane as defined by all landmarks in the configuration (e.g., McNulty et al., 2006; Gunz and Harvati, 2007). Each landmark was averaged with its reflection in order to minimize the effects of bilateral asymmetry, a particularly important step when analyzing fossils (Bookstein, 1996; McNulty et al., 2006). We did not use reconstructed or averaged bilateral landmarks for asymmetry analyses, so as to preserve and quantify differences between antimeres (see below).

Examination of Kabwe revealed that it was missing the outer table and some of the diploë in the region of inion, but did preserve the occipital squama superiorly. Visual examination of other fossil *Homo* specimens after Procrustes superimposition (see below) indicated that La Ferrassie 1 and Saccopastore 1 (not included in this study) exhibited very similar occipital curvature in this region; the average position of inion for these two specimens was used to reconstruct inion for Kabwe. Lambda was difficult to locate in KNM-ER 1813 due to a complicated pattern of sutures and accessory ossicles in the lambdoid region of this fossil (Wood, 1991). A series of semilandmarks was recorded along the midline from glabella to opisthion, and the height of lambda along this curve was estimated in KNM-ER 1813 using five other early *Homo* specimens (KNM-ER 1470, 1805, OH 13, 16, and 24) as a guide (Baab, 2007). A single midline landmark, bregma, was estimated in Zkd 5 using the midsagittal curve of this specimen (the superior portion of which was reconstructed with plaster) and the position of bregma in Zkd 2, 3, 10, 11, and 12 (Baab, 2007). Bregma was then imputed as the closest point on the Zkd 5 midsagittal curve to the mean position of bregma in the Zhoukoudian sample.

As noted by Brown et al. (2004), some standard osteometric landmarks (e.g., lambda and bregma) were difficult to identify in LB1 due to both damage and obliteration of some cranial vault sutures. Therefore, a certain degree of landmark reconstruction was required for this analysis, as is often the case when measuring fossil specimens. For example, information from both the CT scan and from the original specimen (P. Brown, personal communication) regarding the lambdoid sutures were used to establish the position of lambda. Bregma was estimated based on the morphology that was preserved in the surrounding region. Landmarks were excluded from the analysis where damage to the specimen was deemed too extensive for reliable landmark reconstruction, as with the midline of the face.

Generalized Procrustes analysis (GPA) was used to remove nuisance variation due to location, orientation, and scale, although size-correlated shape variation was not removed from the data (Rohlf and Slice, 1990; Rohlf and Marcus, 1993; O'Higgins, 2000; Adams et al., 2004) and forms the basis for these analyses. GPA alignment works by superimposing the centroids of the specimens at a common origin, scaling configurations to a unit centroid size, and then rotating them until the residual sum-of-squares across all landmarks and specimens falls below a set tolerance level (Gower, 1975; Rohlf and Slice, 1990). The landmark configurations for each analysis (i.e., neurocranium + face, neurocranium-only, asymmetry) were superimposed separately. All Procrustes superimpositions were performed in the Morpheus et al. (Slice, 1998) software package. The superimposed coordinates were then treated as shape variables in the statistical analyses described below.

Statistical analysis

As an initial step, we performed separate principal components analyses (PCA) on the shape coordinates for the

Table 2
Landmark definitions and abbreviations.

Landmark/Curve	Abbr.	Definition[a]	Analyses[b]
Dorsal Landmarks			
Inion	IN	The point at which the superior nuchal lines merge in the midline.	NF, N
Lambda	LA	The apex of the occipital bone at its junction with the parietals, in the midline.	N
Bregma	BR	The posterior border of the frontal bone in the midline, taken on the sagittal crest if present.	NF, N
Anterior nasal spine	ANS	Thin projection of bone on the midline at the inferior margin of the nasal aperture.	A[c]
Infraorbital foramen	IF	The most superior point on the infraorbital foramen.	A
Alare	AL	The most lateral point on the margin of the nasal aperture.	NF, A
Zygoorbitale	ZGO	The point where the orbital rim intersects the zygomaticomaxillary suture.	NF, A
Zygomaxillare	ZMO	The most inferior point on the zygomaticomaxillary suture.	A
Dacryon	DA	The point where the lacrimomaxillary suture meets the frontal bone.	NF, A
Supraorbital notch	SON	The point of greatest projection of the notch into the orbital space, taken on the medial edge of the notch.	N
Orbitale	OR	The lowest point on the orbital margin.	A
Frontomalare temporale	FMT	The point where the frontozygomatic suture crosses the temporal line (or outer orbital rim).	NF, N, A
Frontomalare orbitale	FMO	The point where the frontozygomatic suture crosses the inner orbital rim.	NF, N, A
Mid-torus inferior	MTI	The point on the inferior margin of the supraorbital torus, roughly at the middle of the orbit (on the superior margin of orbit).	NF
Mid-torus superior	MTS	The point on the superior aspect of the supraorbital torus, directly above mid-torus inferior on the anterior aspect of the torus.	NF
Anterior pterion	AP	Where the coronal suture intersects the sphenofrontal/sphenoparietal suture.	N
Jugale	JG	The point in the depth of the notch between the temporal and frontal processes of the zygomatic.	NF
Porion	PO	The uppermost point on the margin of the eam.	NF, N
Auriculare	AU	The point vertically above the center of the eam at the root of the zygomatic process.	N
Malar root origin	MR	The point where the malar root arises from the maxilla (often a point of convexity between the molar juga and malar root).	NF, A
Frontotemporale	FT	The point where the temporal line reaches its most anteromedial position on the frontal.	N
Ventral Landmarks			
Opisthion	OP	The midline point at the posterior margin of the foramen magnum.	NF, N
Staphylion	SP	The point on interpalatal suture corresponding to deepest point of notches at the rear of the palate.	A[c]
Midline anterior palatine	MAP	The junction of the palato-maxillary and inter-palatine sutures at midline	A[c]
Incisivion	IV	The midline point at the posterior margin of the incisive foramen (oral).	A[c]
Tympanomastoid junction	TM	The point where the tympanic tube and the mastoid process meet laterally.	N
Postglenoid	PG	The infero-lateral most point posterior to the glenoid fossa and anterior to the ectotympanic tube (corresponds to the postglenoid process).	NF, N
Entoglenoid	EG	The most inferior point on the entoglenoidpyramid.	N
Temporosphenoid suture	TS	The point where the temporosphenoid suture passes from the squama to the cranial base.	N
Lingual canine margin	LC	The most lingual aspect of the canine alveolar process.	NF, A
Canine-P3 contact	C-P3	The contact between the canine and P3 projected onto the buccal alveolar margin.	A
P3-P4 contact	P3-4	The contact between P3 and P4 projected onto the buccal alveolar margin.	A
P4-M1 contact	P4-M1	The contact between P4 and M1 projected onto the buccal alveolar margin.	A
M1-M2 contact	M1-2	The contact between M1 and M2 projected onto the buccal alveolar margin.	NF, A
M2-M3 contact	M2-3	The contact between M2 and M3 projected onto the buccal alveolar surface.	NF, A

[a] Some definitions are modified from Howells (1973), White and Folkens (2000), Frost (2001), and Harvati (2001, 2003). See McNulty (2003) and Baab (2007) for more details.
[b] NF refers to the neurocranium + face analysis, N refers to neurocranium-only analysis, and A refers to the asymmetry analyses.
[c] Refers to midline landmarks used to superimpose specimens for the asymmetry analysis.

neurocranium + face and for the neurocranium-only datasets. We assessed specimen distributions in bivariate plots of principal component (PC) axes, and visualized shape changes associated with each by scaling the eigenvector according to the highest and lowest values on the axis and adding it to and subtracting it from the coordinates of the consensus landmark configuration to generate wireframe models. In landmark-based analyses, this is the visual equivalent of assessing the variable loadings on the eigenvector. The differential weighting of landmarks on each eigenvector was corroborated numerically from the loading scores. Since the variables in this case are the x, y, z coordinates of the landmarks, the influence of any single landmark on an eigenvector was computed as the square root of the sum of the squared coordinate loadings for that landmark (Harvati, 2001). This corresponds precisely to the amount of change in that landmark dictated by the eigenvector. Morphological differences associated with the highest landmark loadings are discussed in the text. All statistical analyses were performed in SAS 8.2 or 9.1 (SAS Institute Inc., Cary, NC); wireframe illustrations were generated using Morpheus et al. (Slice, 1998) and Morphologika[2] v. 2.5 (O'Higgins and Jones, 2006).

An eigenanalysis (PCA) was also performed in Procrustes form (size-shape) space, which incorporates both the shape coordinates and log centroid size as variables. This approach is ideal for examining size-shape relationships (Mitteroecker et al., 2004), and is therefore important here for evaluating size-correlated variation among the crania of humans and African apes. A PCA of only shape variables can confound allometric interpretations among multiple taxa because interspecific variation will typically dominate the first few components while aspects of size-correlated variation get dispersed along multiple PC axes. Since log centroid size usually exhibits substantially more variance than aligned shape coordinates, the addition of this variable to a PCA typically generates a first eigenvector that is predominantly size and its correlated components of shape variation (Mitteroecker et al., 2004). The first component, then, reflects size-correlated shape changes shared among all taxa; subsequent components capture aspects of shape variation not

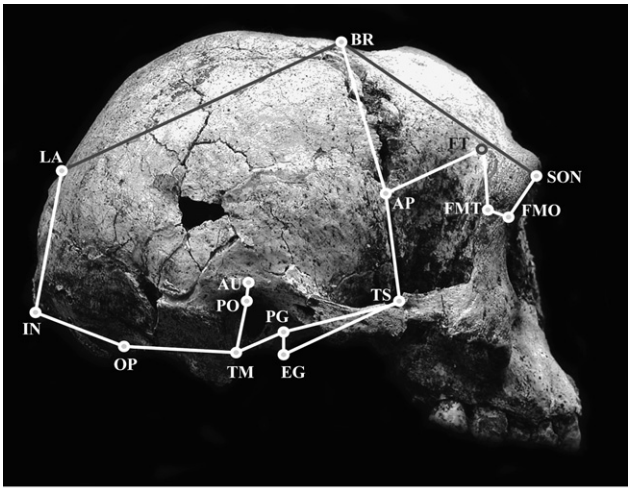

Figure 2. The neurocranium-only landmark set illustrated on the cranium of LB1. The wireframe connecting landmarks is for visualization purposes and does not represent actual data. Landmark abbreviations and definitions can be found in Table 2. The OP, EG, and TS landmarks are not actually visible in this view but their approximate positions are indicated.

correlated with this overall pattern, although they may still exhibit size-shape relationships, particularly *within* individual taxa.

We also used eigenvectors in Procrustes form space to predict the PC scores of an LB1-sized individual based on scores from different taxonomic groups. These groups included Plio-Pleistocene *Homo,* modern humans, australopiths, *Pan paniscus*, *P. troglodytes*, and *G. gorilla* (see Table 1). Scores from individual principal components were regressed on log centroid size and the value for LB1 was compared to the 95% prediction intervals for each group. If the PC scores of LB1 fell within the prediction interval, this was taken as evidence that its cranial shape fit the expected pattern of size-correlated change for that particular group.

To further test whether or not the morphology of LB1 might be reasonably predicted from patterns of static allometry in known groups, morphometric simulations (see McNulty et al., 2006) were generated from multivariate regressions of all shape variables on log centroid size to create hypothetical specimens at the size of LB1. Separate simulations were generated from the modern human sample and the fossil hominin sample. Unlike regressions on single eigenvectors, this procedure incorporated all of the shape variation correlated with size to estimate the landmark configurations of hypothetical individuals with a cranial centroid size equal to that of LB1. Simulations were then compared to the real LB1 specimen by computing the Procrustes distance between them; this metric summarizes overall shape differences as the distance between two configurations in Kendall's shape space (Slice, 2001). Distances between LB1 and the simulations were evaluated against intra-specific variation in Procrustes distances calculated from extant taxa (see McNulty et al., 2006). If the distance between a simulated configuration and LB1 was within the 95% distribution of Procrustes distances in a modern species, this supported the hypothesis that LB1's morphology could be derived from a known human group. If the distance between a hypothetical configuration and LB1 was beyond the 95% distribution, this constituted evidence that size reduction in modern or fossil humans was not sufficient to account for the LB1 morphology. As with the above analyses, separate estimates were made for a combined neurocranium + face dataset and a neurocranium-only set. Fossils used in each analysis are indicated in Table 1.

Finally, two analyses were used to evaluate cranial asymmetry in LB1. First, this was examined in six bilateral landmarks, which correspond generally to the cranial traits studied by Jacob et al. (2006). Table 3 lists the features used in their analysis as well as their analog landmarks (closest 3D equivalent) in this project. Asymmetry was assessed by computing the shortest linear distances from a landmark and its antimere to the midsagittal plane (defined by basion-bregma-staphylion), and then taking the log of the ratio of these distances. While this protocol differs somewhat from the photographic study undertaken by Jacob et al. (2006), the overall approach is similar. Rather than using a clinical standard (see Jacob et al., 2006 and references therein) as the arbiter of abnormal asymmetry, we judged each feature against the degree of asymmetry displayed among extant humans, chimpanzees, bonobos, and gorillas. Apes may provide better benchmarks for the amount of asymmetry expected in early human populations without advanced medical or nutritional knowledge. It should be noted that in most cases, uncertainties pertaining to landmark location are expected to overestimate the degree of observed asymmetry in LB1.

A second assessment of craniofacial asymmetry, incorporating a broader range of landmarks, was also undertaken to compare LB1 to modern taxa and other fossil crania. For this analysis, each specimen configuration was reflected to create a mirror image configuration (e.g., McNulty et al., 2006; Gunz and Harvati, 2007). The entire sample of real and mirrored configurations was superimposed by a GPA of *only the midline landmarks*. This superimposition was accomplished in Morpheus et al. (Slice, 1998) using the "demote" command, which excludes other (non-midline) landmarks from the GPA calculation while rigidly rotating each configuration according to the fitting of the midsagittal landmarks (see McNulty, 2003). This procedure achieved the desired outcome of aligning all specimens on the plane of symmetry, represented as an average of the left and right deviations of the midline landmarks (McNulty, 2003). Once specimens were superimposed in this manner, the overall asymmetry in the configuration was calculated as the generalized Procrustes distance (i.e., without re-aligning specimen pairs) between each specimen and its reflection. By way of explanation, the Procrustes distance between an object and itself is zero; the Procrustes distance between an object and its mirror configuration, therefore, is a measure of that object's asymmetry.

Note that superimposition of mirror configurations based only on midsagittal landmarks can exaggerate asymmetry in bilateral landmarks if the midline points deviate from the true plane of symmetry. This is preferable to using a Procrustes fit of all landmarks, however, because the very goal of superimposition is to minimize those differences in which we are interested. This, in turn, might underestimate the asymmetry in LB1.

As with the previous analysis, this "asymmetric distance" measured between LB1 and its reflection was compared to similar intraspecific values from the extant taxa in order to assess degree of abnormality in the fossil. Additionally, LB1 was compared to other fossil specimens, such as OH 5, Kabwe, and Petralona. Damage and distortion are ubiquitous in the study of fossils, and few specimens survive the fossilization process without incurring some taphonomic alterations. Therefore, a comparative sample of fossils was used to illustrate the asymmetry that might be expected in fossilized cranial specimens.

Table 3
Asymmetric cranial features studied by Jacob et al. (2006) and the corresponding bilateral landmarks assessed in this paper.

Jacob et al., 2006	This Analysis
Maximum cranial breadth	Porion
Orbital lateral rim distance	Frontomalare temporale
Infraorbital foramen distance	Infraorbital foramen
Piriform aperture breadth	Alare
Maxilloalveolar breadth	M2-M3 contact
Maxillary bicanine breadth	Lingual canine margin

Based on the argument that the face of LB1 is particularly asymmetric (Jacob et al., 2006), 34 facial landmarks were used for this second study of asymmetry (see Table 2). Fossil analyses were computed on a reduced subset of 14 facial landmarks due to incomplete bilateral preservation of some specimens.

Results

Principal components analysis of the neurocranium + face landmark set

A standard PCA of the Procrustes aligned coordinates of the neurocranium + face landmark set (illustrated in Fig. 3a and b) included 12 fossil hominins (Table 1). The first component accounted for 81% of the total variance in cranial shape and neatly separated the apes/australopiths from fossil and extant *Homo*. The analysis almost completely divided *H. sapiens* and fossil *Homo*, with the latter group plotting in the direction of the apes. On the first component, LB1 and the Zhoukoudian reconstruction fell at the edge of the modern human distribution in the direction of fossil *Homo* (*H. habilis*, *H. erectus*, and mid-Pleistocene *Homo*). The two groups of short-statured modern humans, the Andaman Islanders and the Khoe-San, clustered together toward the negative pole of PC 2 (along with many average-sized individuals), which explained only 3% of the total variation. LB1, Sangiran 17, and the Zhoukoudian reconstruction all fell within the range of these short-statured populations on PC 2, though only just so in the case of LB1. PC 3 likewise comprised 3% of the total variation, with specimens of fossil *Homo* generally scoring higher on this axis than modern *H. sapiens* (see Fig. 3b). LB1 followed this general trend but, along with Kabwe, Sangiran 17, and the Zhoukoudian reconstruction, was within the modern range.

Shape differences along PC 1 (Fig. 3c) reflected the well-documented differences between apes and modern humans; the apes had longer and more prognathic faces with smaller neurocrania, while humans had greater cranial height, smaller and more orthognathic faces, reduced supraorbital thickness, larger orbits, and wider palates. Accordingly, the landmarks with the greatest influence on the first eigenvector correspond to these differences: inion, bregma, lingual canine margins, opisthion, and the mid-torus landmarks (superior and inferior). Shape differences on PC 2 were related to longer and more orthognathic faces in the higher scoring specimens (Fig. 3d), driven primarily by variation in the palatal landmarks (LC, P4-M1, M1-M2), both mid-torus landmarks, and zygoorbitale. Specimens scoring higher on PC 3 had lower cranial vaults, relatively longer and broader lower faces, and larger orbits (Fig. 3e). Important contributors to this vector were inion, bregma, zygoorbitale, and the lingual canine margins. Interestingly, variability along the first eigenvector was primarily determined by neurocranial landmarks, while facial variability was more prominent on the second PC axis. Both neurocranial and facial landmarks contribute to the shape differences highlighted by PC 3 (Fig. 3e).

Although not shown here, an analysis of only the hominins (excluding the apes) resulted in a similar distribution of specimens along PC 1 (23% of the total variation) and PC 2 (18%). LB1 and the Zhoukoudian reconstruction still overlapped the edge of the modern human range on PC 1. Only the mid-Pleistocene *Homo* fossils were distinct from the modern humans on PC 3 (9%), but fossil *Homo* specimens as a group (including LB1) scored lower than all but the Khoe-San on PC 4 (6%).

Principal components analysis of the neurocranium-only landmark set

Our analysis of the neurocranium-only landmark set incorporated a larger sample of fossil *Homo* specimens than the neurocranium + face analyses, although we excluded the apes and

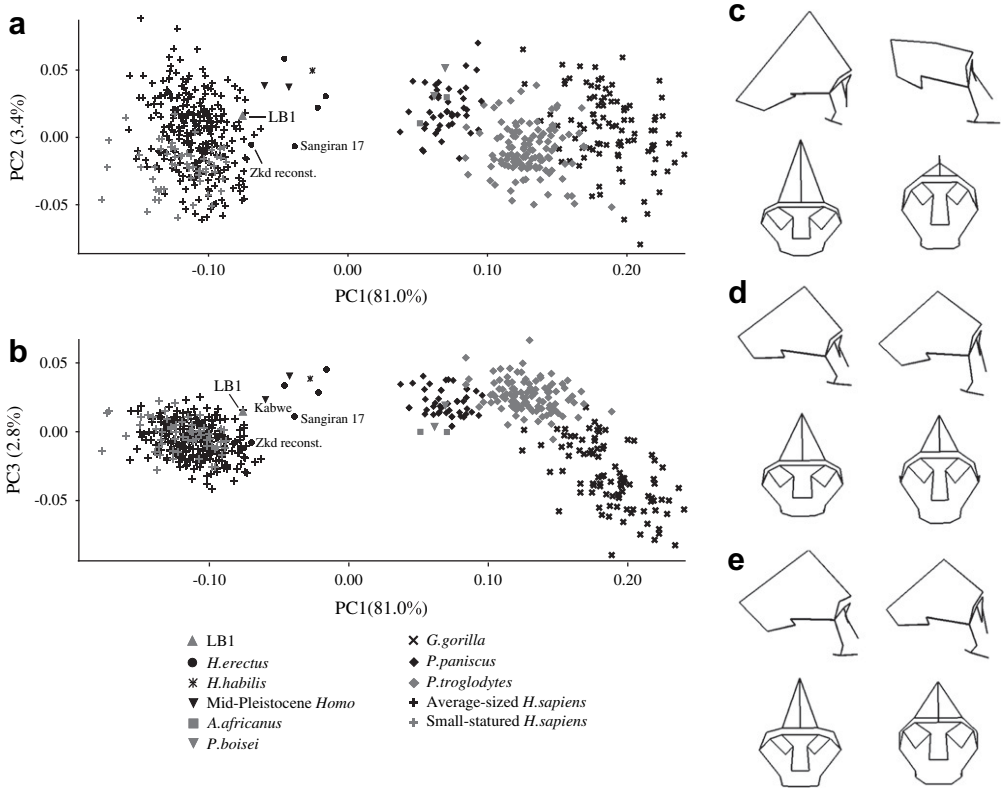

Figure 3. (a) Plot of PC 1 vs. PC 2 and (b) PC 1 vs. PC 3 of neurocranium + face PCA. The cranial shape associated with the negative (left column) and positive (right column) ends of (c) PC 1, (d) PC 2, and (e) PC3, in right lateral and anterior views. Wireframe refers to that illustrated in Fig. 1.

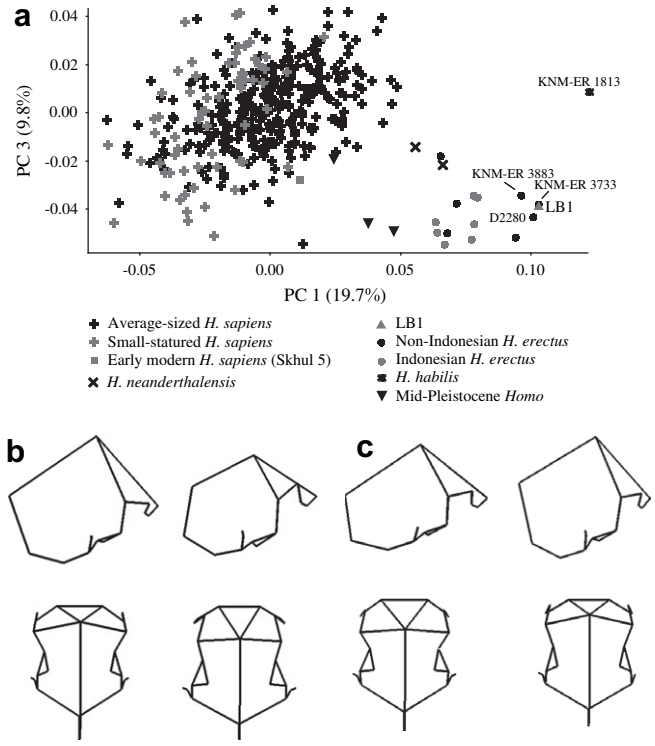

Figure 4. (a) PC 1 vs. PC 3 of neurocranium-only PCA. The shape differences from the negative (left column) to the positive (right column) of (b) PC 1 and (c) PC 3 are shown in right lateral and superior (anterior is facing up) views. Wireframes refer to Fig. 2.

australopiths. Results for PC 1 and 3 were informative (Fig. 4), but PC 2 (not shown) did not help to elucidate group differences. PC 1, which explained approximately one-fifth of the total shape variance, contrasted early *Homo* (*H. habilis* and *H. erectus*) with *H. sapiens*; Neanderthals plotted closer to early *Homo*, while mid-Pleistocene *Homo* overlapped the edge of the modern human range (Fig. 4a). Unlike the PCA of the entire configuration, the neurocranial landmark set clearly distinguished all of the *H. erectus* fossils—along with most of the other fossil specimens—from modern humans. LB1 scored very high on PC 1 and, along with KNM-ER 3733, was the closest specimen to *H. habilis*. While overlapping the modern human range, the fossil specimens (with the exception of *H. habilis*) scored at the negative end of PC 3. Specimens that plotted closest to LB1 on PC 1 and PC 3 were KNM-ER 3733 and KNM-ER 3883 from East Turkana, and D2280 from Dmanisi.

The positive end of PC 1, best represented by KNM-ER 1813, was associated with relatively lower cranial vaults, narrower frontal bones with greater constriction across frontotemporale, more angled occipital bones with shorter upper scales, and more inferiorly projecting entoglenoid processes (Fig. 4b). These shape changes correspond to those landmarks that loaded most strongly on PC 1: lambda, bregma, frontotemporale, inion, and the entoglenoid process. On PC 3 (Fig. 4c), lower-scoring individuals had longer and lower midsagittal cranial profiles, with heavy loadings from lambda, bregma, inion, and the supraorbital notch, and a more superiorly-positioned cranial base (as seen particularly at the tympanomastoid and opisthion landmarks).

Principal components analysis in Procrustes form space of the neurocranium + face landmark set

The major separation in the first two components of Procrustes form space occurred between *Homo* and the African apes, although both groups followed a similar slope on these axes, differing mainly in their intercepts (Fig. 5a). Between these clouds of extant

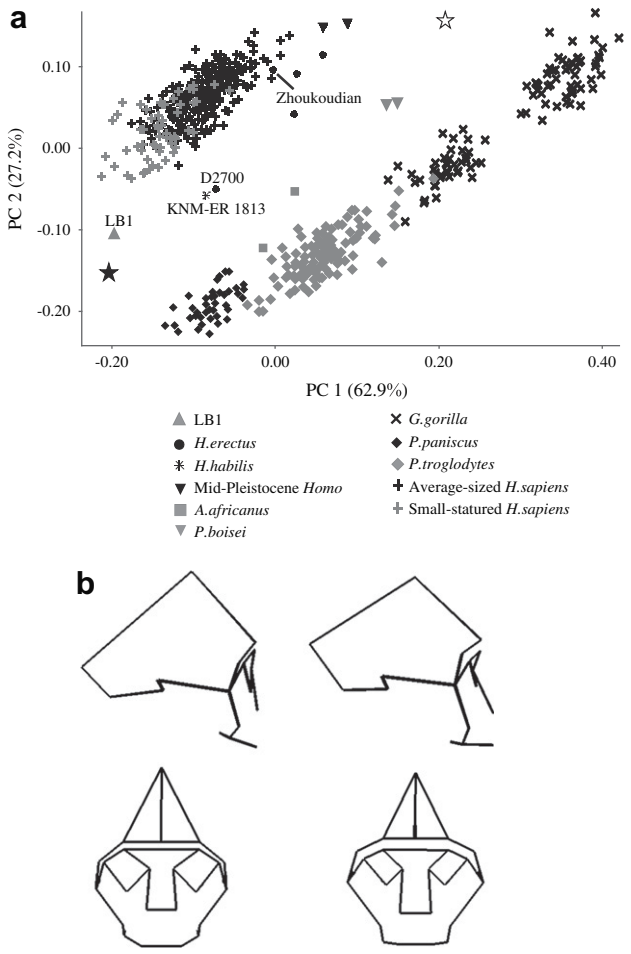

Figure 5. (a) PC 1 vs. PC 2 of PCA in form space of neurocranium + face landmark set. (b) The shape changes associated with smaller (left, solid star) and larger (right, outlined star) specimens in each group are shown in right lateral and anterior views.

specimens were two other groups: fossil *Homo* and australopiths. Both fossil groups also exhibited similar slopes, with *Homo* fossils placed closer to the modern human cluster and australopiths proximate to the ape species. The one interesting exception to this was the Zhoukoudian reconstruction, which plotted just within the bounds of the modern humans. Specimens that scored lower on both PC 1 and PC 2 were the smallest specimens in their respective groups. Therefore, as predicted by their size, the Khoe-San and particularly the Andamanese islanders plotted at the negative end of the modern human distribution. In contrast to these short-statured modern populations, LB1 plotted substantially below the modern human scatter, in line with the slope suggested by the distribution of fossil *Homo*.

The positions of individuals along the first two components were very closely tied to their overall size as indicated by the high coefficients of determination ($R^2 = 0.79–0.99$) within each group (Table 4). Based on these within-group regression equations, we calculated the 95% prediction intervals for PC 1 and PC 2 scores at the LB1 log centroid size in each of these groups (Table 4). The scores of LB1 on the first (−0.198) and second (−0.104) eigenvectors were almost equidistant from predicted values for the modern human and fossil data, but were not within the prediction intervals for either group. While LB1 was closer to the prediction intervals for the group of fossil *Homo*, this interval may be inflated due to the small number of fossil specimens. It is also worth noting that the position of the two small Plio-Pleistocene individuals (KNM-ER 1813 and D2700) strongly influenced the fossil *Homo* slope.

Table 4
Results of regression and prediction calculations for neurocranium + face PCA in form space. PC 1 and PC 2 scores were regressed on log centroid size and these equations were used to predict PC 1 and PC 2 scores at the LB1 centroid size.

Group	PC 1			PC 2		
	p	R^2	Predicted Value (95% Prediction Interval)	p	R^2	Predicted Value (95% Prediction Interval)
Plio-Pleistocene *Homo*	<0.0001	0.97	−0.151 (−0.181/−0.121)	<0.0001	0.98	−0.149 (−0.183/−0.114)
Modern humans	<0.0001	0.87	−0.238 (−0.244/−0.232)	<0.0001	0.87	−0.064 (−0.069/−0.059)
Australopiths	0.0031	0.99	−0.093 (−0.137/−0.050)	0.0023	0.99	−0.191 (−0.231/−0.151)
P. paniscus	<0.0001	0.81	−0.092 (−0.096/−0.088)	<0.0001	0.79	−0.202 (−0.205/−0.199)
P. troglodytes	<0.0001	0.89	−0.068 (−0.076/−0.060)	<0.0001	0.87	−0.225 (−0.232/−0.217)
G. gorilla	<0.0001	0.97	−0.060 (−0.073/−0.047)	<0.0001	0.96	−0.234 (−0.245/−0.222)
			PC 1 Score			PC 2 Score
LB1			−0.198			−0.104

Figure 5b illustrates the shape differences on the combined first two axes represented by the two stars. Smaller specimens in each of these groups had slightly larger neurocrania relative to the face with increased height at bregma and reduced prognathism in the lower face. Additionally, facial height shortened, the supraorbital torus was reduced, the orbits were larger, and the palate widened in these smaller specimens. For both axes, the highest loadings were from inion, bregma, the lingual canine margin, and opisthion.

Principal components analysis in Procrustes form space of the neurocranium-only landmark set

The Procrustes form analysis for the neurocranium-only landmarks indicated substantial overlap of modern and fossil humans on the first component but good separation on PC 2 (see Fig. 6a).

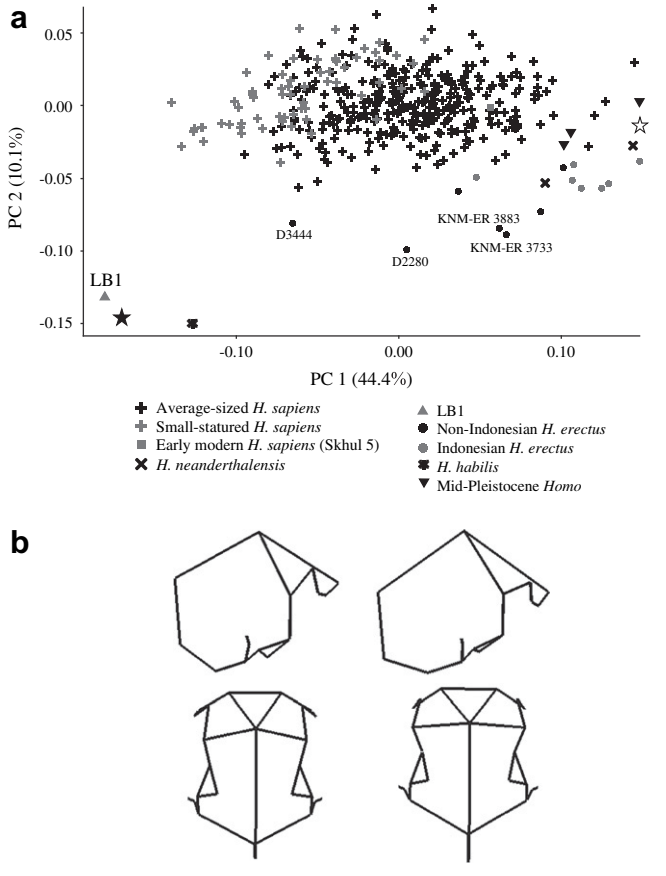

Figure 6. (a) PC 1 vs. PC 2 of PCA in form space of neurocranium-only landmark set. (b) The shape changes associated with smaller (left, solid star) and larger (right, outlined star) Plio-Pleistocene hominins are shown in right lateral and anterior views.

LB1 fell closest to KNM-ER 1813 in this analysis and both were well separated from the other archaic *Homo* specimens and from modern humans. The slope observed in the Plio-Pleistocene *Homo* group reflects the influence of size on both PC 1 and PC 2 in this group (Table 5). Importantly, this slope did not parallel the modern human trend, which varied along the second eigenvector according to population and individual differences to a greater degree than size (Table 5). Shape differences shown in Fig. 6b specifically illustrate changes along the slope of the fossil *Homo* specimens (between the two stars). For individuals scoring low on both axes (= smaller cranial size), these included less height at bregma, a more antero-superiorly positioned lambda and inion, more inferiorly projecting entoglenoid processes, more postero-superiorly positioned frontotemporale, and less breadth across anterior pterion. The differences correspond to heavy loadings from lambda, bregma, frontotemporale, and inion on both axes. Slightly subordinate loadings were also found at auriculare and porion on the first axis, and at the entoglenoid process on the second.

Log centroid size accounted for nearly all variation in PC 1 scores for both modern humans ($R^2 = 0.99$) and Plio-Pleistocene *Homo* ($R^2 = 0.99$) (Table 5). Although there was also a statistically significant relationship between size and PC 2 scores in both groups, size only accounted for a meaningful proportion of variation in the Plio-Pleistocene *Homo* group (72% vs. 2% in modern humans). This suggests that the pattern of size-correlated shape variation in the neurocranium of modern humans has departed from the general pattern found in archaic species of *Homo*.

When the PC 1 and PC 2 scores of modern humans and Plio-Pleistocene *Homo* were regressed on log centroid size, the observed scores for LB1 fell within the 95% prediction interval for Plio-Pleistocene *Homo* on both axes (PC 1 = −0.182, PC 2 = −0.131), but beyond the intervals predicted for modern humans. Hence, LB1 adheres to the pattern of static allometry estimated from neurocranial shape in archaic *Homo*. Although not shown here, if mid-Pleistocene *Homo* specimens are excluded from the Plio-Pleistocene regression (given their overlap with modern humans), this result remains unchanged. Similarly, excluding KNM-ER 1813, which had a strong effect on the regression slope, did not affect this prediction result.

Morphometric simulations based on patterns of static allometry

Morphometric simulations allowed us to test whether or not the LB1 morphology represents a small version of extant or fossil hominins. We conducted multivariate regressions of all shape coordinates on log centroid size to simulate hypothetical landmark configurations at the centroid size of LB1. Based on static allometry models, these hypothetical specimens represent the cranial shape one might expect in either modern or fossil *Homo* of this diminutive size.

Comparisons of the simulated specimens to LB1 are illustrated for both the neurocranium + face and the neurocranium-only

Table 5
Results of regression and prediction calculations for neurocranium-only PCA in form space. PC 1 and PC 2 score were regressed on log centroid size and these equations were used to predict PC 1 and PC 2 scores at the LB1 centroid size.

Group	PC 1			PC 2		
	p	R^2	Predicted Value (95% Prediction Interval)	*p*	R^2	Predicted Value (95% Prediction Interval)
Plio-Pleistocene *Homo*	<0.0001	0.99	−0.182 (−0.190/−0.174[a])	<0.0001	0.72	−0.160 (−0.193/−0.127[a])
Modern humans	<0.0001	0.99	−0.219 (−0.221/−0.217)	0.0115	0.02	−0.009 (−0.018/0.000)
			PC 1 Score			PC 2 Score
LB1			−0.182			−0.131

[a] Indicates that the actual values for LB1 fit within the 95% prediction interval.

models (Figs. 7 and 8). In the neurocranium + face analysis, the Procrustes distance between LB1 and the fossil hominin simulation (0.0960) fell within the 95% limit of intraspecific distances observed in all four extant species (Table 6). The modern human simulation was less similar to LB1, with a Procrustes distance (0.1281) that could only be accommodated in the range of *G. gorilla* variability.

These results suggest that the shape of the LB1 cranium largely reflects the expected shape of a fossil hominin writ small; the case for LB1 representing a scaled-down modern human was supported here only if one accepts the highly variable gorilla model (e.g., Harvati et al., 2004; Miller et al., 2004; McNulty et al., 2006; Baab, 2008; see Groves, 2001) as the appropriate standard. In fact, when gorilla males and females were analyzed separately, their 95% upper limits (male = 0.1216; female = 0.1067) also excluded the modern human simulation, illustrating the influence of sexual dimorphism on Procrustes distances in *G. gorilla*. Even accepting the gorilla model as appropriate, it is clear that the simulation produced from fossil hominins provides a far better estimate of the LB1 morphology than does the modern human estimate.

Similar results were obtained in the neurocranium-only analysis, although the different landmark set precluded inclusion of the ape species. The simulation produced from the fossil human sample was very similar to the LB1 neurocranium, with a Procrustes distance (0.0998) well within the standard of intraspecific variation for modern humans. The Procrustes distance between the modern human simulation (0.1661) and LB1, however, was more than five standard deviations from the mean distance in the modern humans, making it a very poor predictor of the LB1 morphology.

Cranial asymmetry

The 3D data collected here were also useful in addressing whether or not LB1 was pathologically asymmetric. We initially analyzed six bilateral landmarks chosen to represent morphology also studied by Jacob et al. (2006; see Table 3). While the methods used here were broadly similar to those used in that study, it is important to note that our landmarks and methods did not exactly reproduce the 2D image analysis described by Jacob et al. (2006), which could explain any differences in our results.

This first asymmetry analysis showed that distances of three bilateral landmarks (porion, frontomalare temporale, and M2-M3 contact) to the midline deviated only slightly from perfect symmetry (Table 7). With the exception of porion, these were well within one standard deviation (SD) of observed asymmetry in all four extant species; porion was within two SD compared with bonobos as a result of the unusually high asymmetry of porion in *P. paniscus* rather than LB1 (Table 7). The placement in LB1 of the infraorbital foramina, alare, and the lingual canine margins were far more asymmetric, but matched tendencies in extant species. For that reason, the asymmetry values for infraorbital foramen and alare in LB1 are still within two SD of the asymmetry found in either species of *Pan* and within one SD of the gorilla and modern human

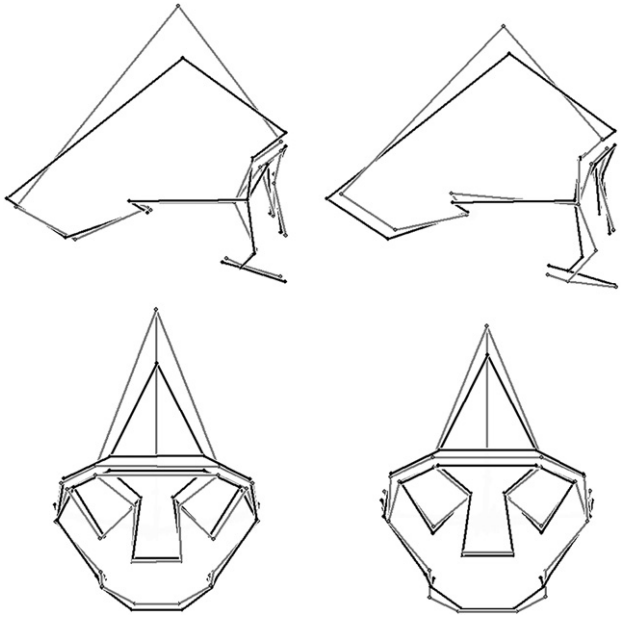

Figure 7. The simulated cranial (neurocranium + face) shape of modern humans (left) and Plio-Pleistocene *Homo* (right) at the same log centroid size as LB1, compared to the actual LB1 cranial shape in right lateral and anterior views. The black wireframe is LB1 and the gray wireframes are the simulations.

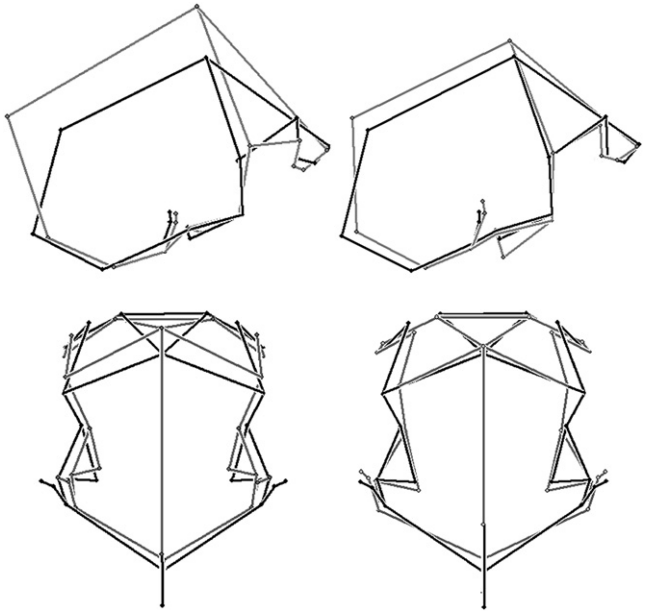

Figure 8. The simulated neurocranial shape of modern humans (left) and Plio-Pleistocene *Homo* (right) at the same log centroid size as LB1, compared to the actual LB1 cranial shape in right lateral and superior views. The black wireframe is LB1 and the gray wireframes are the simulations.

Table 6
Procrustes distances: a) between simulated scaled down configurations and the LB1 cranium for the neurocranium + face and neurocranium-only analyses, and b) within species of extant apes and humans.

	Neurocranium + face			Neurocranium only		
a)						
	Procrustes distance to LB1			Procrustes distance to LB1		
Modern human simulation	0.1281			0.1661		
Plio-Pleistocene *Homo* simulation	0.0960			0.0998		
b)						
Species	mean	sd	95% upper limit	mean	sd	95% upper limit
Modern humans	0.0824	0.0173	0.1171	0.0791	0.0162	0.1115
P. paniscus	0.0695	0.0166	0.0976	–	–	–
P. troglodytes	0.0766	0.0144	0.1055	–	–	–
G. gorilla	0.1001	0.0226	0.1454	–	–	–

values. The landmark exhibiting the greatest asymmetry in LB1 (0.3945), and in all four extant species, was the lingual canine margin (cf. "maxillary bicanine breadth" in Jacob et al., 2006). This value was nevertheless within two SD when compared to gorillas, modern humans, and *P. troglodytes*, but beyond two SD with *P. paniscus* as the benchmark.

A more general analysis of asymmetry examined 34 facial landmarks to compare LB1 to extant taxa, and then a subset of 14 landmarks so as to include several fossil comparators (Fig. 9). Based on the Procrustes distances between each specimen configuration and its bilaterally reflected configuration, the LB1 fossil is highly asymmetrical when compared to extant taxa (Fig. 9a). This value was nevertheless well within the ranges exhibited by all four extant species, and within the upper whisker limits (1.5 interquartile ranges) of all but modern humans. Thus, the degree of asymmetry in LB1 was not beyond empirically observed limits established by other hominines. Moreover, other fossils were also highly asymmetrical, and the LB1 value was lower (more symmetrical) than the Kabwe, Bodo, and Arago crania (but higher than OH 5, Petralona, Abri Pataud, and Fish Hoek) (Fig. 9b). In this case, as with most fossil crania, asymmetry in LB1 is likely a consequence of taphonomy instead of pathology.

Discussion

Static allometry and hominin cranial variation

Our quantitative analyses show that the morphology of the LB1 cranium is consistent with the expected shape for a very small specimen of archaic *Homo*. This is particularly salient in the neurocranium, for which congruent results were obtained from PCAs in shape and Procrustes form spaces as well as from morphometric simulations. When facial landmarks are included, LB1 fits neither the modern nor archaic predictive models on the first two component axes of Procrustes form space. Nevertheless, it is clearly distinct from the modern human sample in this analysis (Fig. 5a). Moreover, morphometric simulations with the facial landmarks included—which have the advantage of incorporating all of the shape variables—demonstrate that LB1 *does* fit the pattern of size-correlated shape change observed in fossil *Homo*. Our results are also consistent with two previous analyses based on linear measurements of the cranium (Argue et al., 2006; Gordon et al., 2008), and support the hypothesis that that the Flores hominins were diminutive representatives of a species of archaic *Homo*.

Results from the PCA of the entire landmark set may lead one to reject this conclusion as LB1 is clearly within the modern human range, albeit on the periphery, for the component that best separates extant and fossil *Homo* (Fig. 3). However, the similarities between LB1 and modern humans take on a new significance after considering carefully the patterns of static allometry also presented in this study. In Procrustes form analysis, a common pattern of size-correlated shape change is observed in both humans and apes, with fossil specimens, including LB1, adhering to this trend but clustering between the two extant distributions (see Fig. 5). Morphological changes associated with size reduction include reduced facial height, larger orbits, decreased supraorbital thickness, and a broadening of the palate. These same characteristics distinguish modern humans from fossil humans and apes along PC 1 of the original PCA (compare Figs. 3c and 5b). In other words, the shared pattern of shape change correlated with size reduction includes several facial features that also align LB1 with modern humans (Fig. 3). This has critical implications for interpreting the LB1 morphology, as many of its modern features (see Jacob et al., 2006) might also be expected in an archaic species of that size.

There has been a great deal of debate over whether or not a condition of microcephaly may be causing some researchers to assign LB1 incorrectly to a new species, *H. floresiensis* (Brown et al., 2004; Henneberg and Thorne, 2004; Falk et al., 2005, 2006, 2007; Morwood et al., 2005; Weber et al., 2005; Argue et al., 2006; Jacob et al., 2006; Martin et al., 2006a,b; Richards, 2006). Absent from this conversation has been the equally valid concern that the small size of LB1 may instead lead researchers to erroneously associate it with modern humans. Our analysis indicates that this latter concern is a distinct possibility when patterns of static allometry are not taken into consideration.

Table 7
Asymmetry in six bilateral landmarks, assessed by computing the shortest linear distances from a landmark and its antimere to the midsagittal plane, and then taking the log of the ratio of these distances. A value of zero, therefore, would represent perfect symmetry. The first results column gives the asymmetry in LB1 for each landmark. Each additional group of columns gives mean values and standard deviations of the logged ratios in extant taxa, as well as the degree of asymmetry in LB1 in terms of the extant standard deviations. Landmark abbreviations are given in Table 2.

	LB1	Gorilla			Modern Human			Chimpanzee			Bonobo		
		mean	sd	LB1	mean	sd	LB1	mean	sd	LB1	mean	sd	LB1
PO	−0.0121	0.0128	0.0422	<1 sd	0.0063	0.0432	<1 sd	0.0089	0.0394	<1 sd	0.04854	0.0411	<2 sd
FMT	−0.0021	−0.0042	0.0662	<1 sd	0.0356	0.0635	<1 sd	−0.0254	0.0586	<1 sd	−0.01824	0.0437	<1 sd
IF	0.1375	0.0289	0.1171	<1 sd	0.0723	0.1052	<1 sd	0.0106	0.0880	<2 sd	−0.00095	0.0848	<2 sd
AL	0.2549	0.0498	0.2715	<1 sd	0.1889	0.2413	<1 sd	0.0288	0.2088	<2 sd	0.01528	0.2090	<2 sd
M2-3	0.0261	0.0545	0.0711	<1 sd	0.0365	0.0556	<1 sd	0.0617	0.0674	<1 sd	0.01939	0.0612	<1 sd
LC	0.3945	0.1120	0.2661	<2 sd	0.0810	0.2101	<2 sd	0.0996	0.1660	<2 sd	0.03806	0.1751	<3 sd

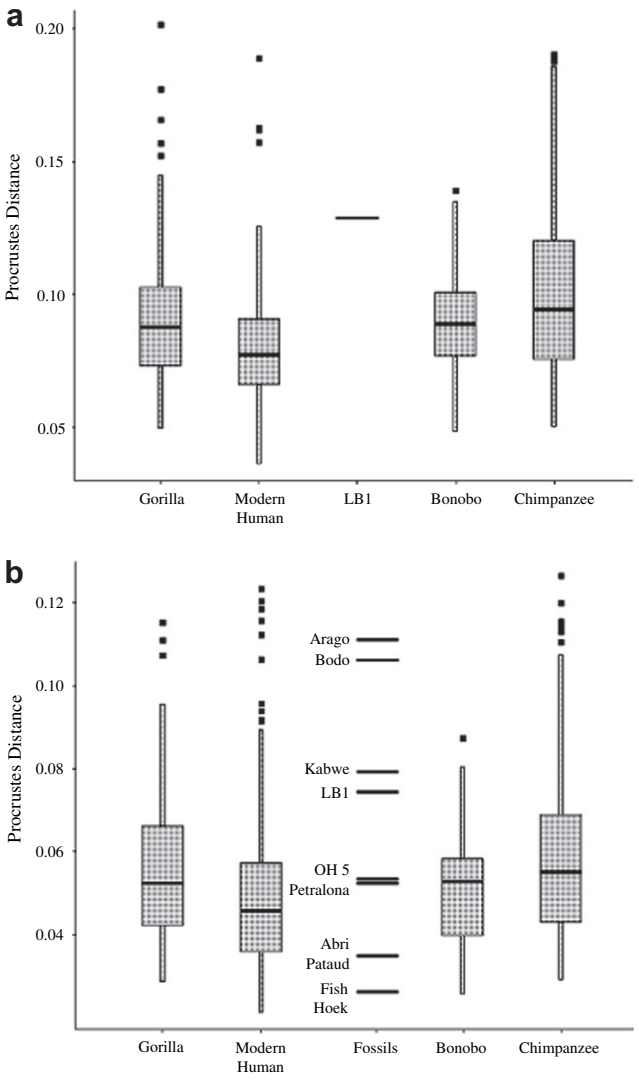

Figure 9. Degree of asymmetry in extant taxa and fossil hominins calculated as the Procrustes distance between each specimen and its reflected configuration: a) based on 34 facial landmarks comparing asymmetry in LB1 to that present in extant species; b) based on 14 facial landmarks comparing LB1 to other fossil hominins as well as to extant species.

Size-related variation matter less when analyses are restricted only to neurocranial landmarks, because the differences in vault morphology that separate fossil and modern humans are not coincident with observed patterns of size-correlated variation. In Procrustes form space, the archaic *Homo* sample shows a clear pattern of static allometry (see Table 5). The nature of this size-correlated shape change differs in several ways from the pattern that unites LB1 with the fossil specimens (compare Figs. 4b and 6b). Consequently, LB1's neurocranial affinities to *H. erectus* and other Plio-Pleistocene hominins cannot simply be attributed to the effects of size reduction. Also of particular interest is the distribution of modern humans in this Procrustes form space analysis. Unlike size-correlated variation in their fossil counterparts, this variation in extant humans was partitioned almost exclusively on the first axis. Partitioning along the first axis reveals that the observed pattern of static allometry in the neurocrania of modern humans differs from a more common trend shared among these fossils. Together, these results suggest that neurocranial morphology (here including both neurocranial and basicranial landmarks) may provide a better estimate of relationships among hominins of very different body sizes than does overall cranial morphology.

Our results compare favorably with other multivariate analyses of the LB1 cranium (Argue et al., 2006; Gordon et al., 2008) in positioning this specimen closest to *H. erectus* (*s.l.*), particularly the early African forms. Gordon et al. (2008) also explicitly considered the effects of size on cranial shape, concluding that LB1 most closely resembled non-Asian *H. erectus* when accounting for size. Note that several of the measurements used by Gordon et al. (2008) were based on estimates of midline facial landmarks (i.e., glabella, nasion, and prosthion) that were not analyzed here. The fact that both studies reached similar conclusions based on different cranial measures emphasizes that the affinities of LB1 lie with archaic *Homo* when its small size is considered quantitatively.

Asymmetry in the LB1 cranium

Substantial asymmetry occurs in the LB1 cranium, and while it may be technically correct that asymmetry in this fossil "exceeds clinical norms" (Jacob et al., 2006: 13423), our results show that the degree of asymmetry is within the overall ranges of modern humans and apes. Environmental perturbations leading to systemic stress are often implicated in increased levels of asymmetry (Siegel et al., 1977; Doyle and Johnston, 1977; Sciulli et al., 1979; Swaddle and Witter, 1994; DeLeon, 2007); the lower values of asymmetry in the modern human sample evident from this analysis might be expected as a result of improved medical and nutritional knowledge, which should increase developmental stability. When compared to non-human African apes, however, the asymmetry in LB1 is reasonably accommodated within normal variability. Alternatively, taphonomic processes have distorted the original morphology of many fossils. Thus, while our results confirm that LB1 is asymmetric in several aspects of its cranial morphology, we do not find the degree of difference to be beyond what might be expected in an archaic hominin population, particularly considering taphonomic processes.

Implications for the evolutionary history of the Flores hominins

The broader implications of this project support two likely scenarios: 1) *H. floresiensis* was the end product of size reduction of an existing archaic *Homo* species, or 2) *H. floresiensis* was part of a longer-lived, but currently-unidentified lineage of small-statured and small-brained *Homo*. As even the smallest early *Homo* and *H. erectus* fossils are significantly larger than *H. floresiensis*, some process of diminution likely occurred in the latter's evolutionary history. Given our findings, hypotheses that posit at least some size reduction are therefore the most parsimonious, but not exclusive, explanations for the morphology of LB1. This does not require that size reduction occurred in isolation on Flores, but the presence of dwarfed *Stegodon* (van den Bergh et al., 2009) offers evidence that this environment was compatible with the process of nanism.

The overall shape of the LB1 neurocranium fits well within the range of variation for fossil *Homo*, with greatest similarities to early African/Georgian *H. erectus* (see also Brown et al., 2004; Argue et al., 2006; Gordon et al., 2008). Limited evidence supports the presence of more primitive, and possibly smaller, forms of *H. erectus*, both at Dmanisi (Gabounia et al., 2000, 2002; Vekua et al., 2002; Lordkipanidze et al., 2005, 2007) and on Java in the early Pleistocene (Kaifu et al., 2005; Baab, 2007). Dispersals predating *H. erectus* from Africa have also been proposed (e.g., Clarke, 1990, 2000; Swisher et al., 1994; White, 1995; Wang and Tobias, 2001; Asfaw et al., 2002; Dennell and Roebroeks, 2005). Much of the postcranial evidence from Liang Bua supports dispersal of a fairly primitive hominin from Africa (e.g., Tocheri et al., 2007). While LB1 closely resembles D2280 and D2700 (unpublished data) from Dmanisi in its overall

neurocranial shape, comparisons between the Dmanisi and Liang Bua postcrania are not yet available and there are no postcranial remains from the earliest levels of the Sangiran Formation. Despite some postcranial and mandibular similarities with the australopiths, LB1 does not resemble *A. africanus* in any aspects of its cranial shape.

Studies that support a hypothesis of microcephaly for LB1 have focused on a number of issues involving brain size to body size scaling and pathologies of the postcranial skeleton (Martin et al., 2006a,b; Jacob et al., 2006; Richards, 2006), while paying less attention to details of the cranial morphology of LB1 that link it to archaic hominins. Both Jacob et al. (2006) and Richards (2006) argued that the LB1 cranium included individual features observed among widely distributed modern humans, particularly in modern Southeast Asians. However, neither study addressed the probability of finding the *suite* of features present in LB1 in a modern human population. Our explicitly multivariate approach, especially the neurocranial PCA, clearly indicates that the shape of the LB1 vault falls outside the range of modern humans. Instead, it fits a pattern of size and shape variation in early *H. erectus*, and to a lesser extent *H. habilis*. The presence or absence of single characters in a geographically far-flung species like *H. sapiens*, therefore, constitutes poor evidence that LB1 was also a member of this species. The total pattern of neurocranial shape, including the low cranial profile, projecting occipital, tall supraorbital torus, wide posterior neurocranium, and narrow frontal bone with greater constriction across frontotemporale, is more consistent with fossil *Homo* than modern humans.

Richards (2006) also suggested that the seemingly archaic nature of LB1 might be the direct result of a modern human population becoming smaller in an island setting. Results of the size-shape analyses suggest otherwise; small modern humans do not more closely resemble *H. erectus* or LB1 than do larger modern humans. In fact, our results for modern *H. sapiens* neurocrania (captured by PC 1 of Procrustes form space) indicate that those with smaller skulls are relatively taller at bregma, less projecting posteriorly, and have wider frontal bones compared to those with larger skulls. This is opposite to the pattern observed in the LB1 cranium. Rather than size reduction causing modern humans to look more archaic, it is clear from results presented here that size reduction instead causes archaic facial morphology to look more modern, at least in certain respects.

Conclusions

The cranial morphology of LB1 clearly aligns it with the genus *Homo*, even though LB1 is smaller in both body and brain size than any other members of our genus. This implies that some form of diminution occurred in the evolutionary history of *H. floresiensis*. This study found a shared pattern of size-related cranial shape variation across hominines, including both extant and fossil hominins. Based on this pattern, this study further found that the cranial shape of LB1 largely fit a model for a small specimen of archaic *Homo*. In contrast, it does not resemble a small modern human. If this basic relationship between cranial size and shape accounts for the observed morphology of LB1, then it is unnecessary to postulate additional factors, such as microcephaly, in the absence of strong evidence to support such a claim.

Analyses of bilateral cranial features revealed asymmetry levels in LB1 consistent with the degree of asymmetry found in extant apes and humans. Additionally, an overall assessment of facial asymmetry found that LB1 is well within ranges observed among extant hominines, and less asymmetric than some other fossil *Homo* crania. As with most of the specimens recovered by paleoanthropologists, the most likely causes of asymmetry in LB1 were post-mortem taphonomic processes rather than developmental abnormalities.

The numerous primitive features of the mandible (Brown, 2009) and postcranial skeleton (Brown et al., 2004; Morwood et al., 2005; Argue et al., 2006; Larson et al., 2007; Tocheri et al., 2007; Jungers et al., 2008), combined with the shape of the cranium, suggest that the ancestor of *H. floresiensis* was more primitive than the majority of Asian *H. erectus* specimens, perhaps resembling the oldest Sangiran dome fossils (Kaifu et al., 2005). Here, the overall shape of the LB1 cranial vault was most similar to the East Turkana hominins and D2280 from Dmanisi (see also Brown et al., 2004; Argue et al., 2006). These results concur with the hypothesis that the Liang Bua fossils may have descended from a hominin population more primitive than Asian *H. erectus* that underwent a process of size reduction.

Acknowledgements

The authors appreciate the assistance of the following individuals in the preparation of this manuscript: Peter Brown, Eric Delson, Ryan Raaum, Steve Frost, Will Harcourt-Smith, and Jim Rohlf. We also thank Tony Djubiantono and ARKANAS for access to the Liang Bua material, and Mike Morwood and William Jungers for inviting us to contribute to this special volume on the Liang Bua hominins. We thank Steven Leigh, William Jungers, Adam Gordon, and Katerina Harvati for their comments on this manuscript. We gratefully acknowledge the curators and staff of the American Museum of Natural History, Aristotle University of Thessaloniki, Duckworth Collection at the University of Cambridge, Gadja Mada University, Humboldt University Museum, LIPI, Musée de L'Homme, Musée Royal de l'Afrique Centrale, National Museums of Ethiopia, National Museums of Kenya, National Museum of Tanzania, COSTECH, Natural History Museum, Museum of Comparative Zoology, Peabody Museum at Harvard University, Powell-Cotton Museum, University of Cape Town, and the Institut de Paléontologie Humaine for allowing us access to fossil and comparative samples. Grant support was provided by NSF (BCS 04-24262, DGE 03-33415, and DBI 96-02234), the L.S.B. Leakey Foundation, and the Sigma Xi Foundation. This is NYCEP morphometrics contribution number 28.

References

Adams, D.C., Rohlf, F.J., Slice, D.E., 2004. Geometric morphometrics: ten years of progress following the 'revolution'. Ital. J. Zool. 71, 5–16.

Andrews, P., 1984. An alternative interpretation of the characters used to define *Homo erectus*. Cour. Forsch.-Inst. Senckenberg 69, 167–175.

Antón, S.C., 2001. Cranial growth in *Homo erectus*. In: Minugh-Purvis, N., McNamara, K.J. (Eds.), Human Evolution Through Developmental Change. Johns Hopkins University Press, Baltimore, pp. 349–380.

Antón, S.C., 2003. Natural history of *Homo erectus*. Yearb. Phys. Anthropol. 46, 126–170.

Argue, D., Donlon, D., Groves, C., Wright, R., 2006. *Homo floresiensis*: microcephalic, pygmoid, *Australopithecus*, or *Homo?* J. Hum. Evol. 51, 360–374.

Asfaw, B., Gilbert, W.H., Beyene, Y., Hart, W.K., Renne, P.R., WoldeGabriel, G., Vrba, E.S., White, T.D., 2002. Remains of *Homo erectus* from Bouri, Middle Awash, Ethiopia. Nature 416 317–320.

Azzaroli, A., 1981. About pygmy mammoths of the Northern Channel Islands and other island faunas. Mem. Soc. Geol. Fr. 16, 423–425.

Baab, K.L., 2007. Cranial shape variation in *Homo erectus*. Ph.D. Dissertation, City University of New York.

Baab, K.L., 2008. The taxonomic implications of cranial shape variation in *Homo erectus*. J. Hum. Evol. 54, 827–847.

Baab, K.L. Cranial shape in Asian *Homo erectus*: geographic, anagenetic, and size-related variation. In: Norton, C.J., Braun, D.R., Harris, J.W.K. (Eds.), Asian Paleoanthropology: From Africa to China and Beyond. Springer, in press.

Baab, K.L., McNulty, K.P., Brown, P., 2007. Allometric scaling of craniofacial shape: implications for the Liang Bua hominins. PaleoAnthropology 2007, A2.

Barker, G., 2002. Prehistoric foragers and farmers in South-east Asia: renewed investigations at Niah Cave, Sarawak. P. Prehist. Soc. 68, 147–164.

Bartstra, G.J., Soegondho, S., van der Wijk, A., 1988. Ngandong man: age and artifacts. J. Hum. Evol. 17, 325–337.

Black, D., 1929. Preliminary notice of the discovery of an adult *Sinanthropus* skull at Chou Kou Tien. Bull. Geol. Soc. China 8, 15–32.

Black, D., 1931. On an adolescent skull of *Sinanthropus pekinensis* in comparison with an adult skull of the same species and with other hominid skulls, recent and fossil. Palaeontologica Sinica Ser. D 7, 1–144.
Bookstein, F.L., 1996. Combining the tools of geometric morphometrics. In: Marcus, L.F., Corti, M., Loy, A., Naylor, G.J.P., Slice, D.E. (Eds.), Advances in Morphometrics. Kluwer Academic Publishers, Netherlands, pp. 131–151.
Brandon-Jones, D., 1998. Pre-glacial Bornean primate impoverishment and Wallace's line. In: Hall, R., Holloway, J.D. (Eds.), Biogeography and Geological Evolution of Southeast Asia. Backhuys Publishers, Leiden, pp. 393–404.
Brown, P., Maeda, T., 2009. Liang Bua *Homo floresiensis* mandibles and mandibular teeth: a contribution to the comparative morphology of a new hominin species. J. Hum. Evol. 57 (5), 571–596.
Brown, P., Sutikna, T., Morwood, M.J., Soejono, R.P., Jatmiko, Saptomo, E.W., Rokus Awe Due, 2004. A new small-bodied hominin from the Late Pleistocene of Flores, Indonesia. Nature 431, 1055–1061.
Brumm, A., Aziz, F., Van den Bergh, G.D., Morwood, M.J., Moore, M.W., Kurniawan, I., Hobbs, D.R., Fullager, R., 2006. Early stone technology on Flores and its implications for *Homo floresiensis*. Nature 441, 624–628.
Cavalli-Sforza, L.L., 1986. African Pygmies: an evaluation of the state of research. In: Cavalli-Sforza, L.L. (Ed.), African Pygmies. Academic Press, Orlando, pp. 81–93.
Clarke, R.J., 1990. The Ndutu cranium and the origin of *Homo sapiens*. J. Hum. Evol. 19, 699–736.
Clarke, R.J., 2000. Out of Africa and back again. Int. J. Anthropol. 15, 185–189.
Cox, C.B., 2000. Plate tectonics, seaways and climate in the historical biogeography of mammals. Memórias do Instituto Oswaldo Cruz 95, 509–516.
Davis, S., 1985. Tiny elephants and giant mice. New Scientist 105, 25–27.
DeLeon, V.B., 2007. Fluctuating asymmetry and stress in a Medieval Nubian population. Am. J. Phys. Anthropol. 132, 520–534.
Dennell, R., Roebroeks, W., 2005. An Asian perspective on early human dispersal from Africa. Nature 438, 1099–1104.
Dennell, R.W., 2005. The Solo (Ngandong) *Homo erectus* assemblage: a taphonomic assessment. Archaeology in Oceania 40, 81–90.
Doyle, W.J., Johnston, O., 1977. On the meaning of increased fluctuating dental asymmetry: a cross populational study. Am. J. Phys. Anthropol. 46, 127–134.
Falk, D., Hildebolt, C., Smith, K., Jungers, W.L., Larson, S.G., Morwood, M.J., Sutikna, T., JatmikoSaptomo, E.W., Prior, F., 2008. LB1 did not have Laron syndrome. Am. J. Phys. Anthropol. 135, 95 (Abstract).
Falk, D., Hildebolt, C., Smith, K., Morwood, M.J., Sutikna, T., Brown, P., Jatmiko, E., Saptomo, Wayhu, Brunsden, B., Prior, F., 2005. The brain of LB1, *Homo floresiensis*. Science 308, 242–245.
Falk, D., Hildebolt, C., Smith, K., Morwood, M.J., Sutikna, T., Jatmiko, Saptomo, E.W., Brunsden, B., Prior, F., 2006. Response to Comment on "The Brain of LB1, *Homo floresiensis*". Science 312 999c.
Falk, D., Hildebolt, C., Smith, K., Morwood, M.J., Sutikna, T., Jatmiko, Saptomo, E.W., Imhof, H., Seidler, H., Prior, F., 2007. Brain shape in human microcephalics and *Homo floresiensis*. Proc. Natl. Acad. Sci. USA 7, 2513–2518.
Franzen, J.L., 1985. Asian australopithecines? In: Tobias, P.V. (Ed.), Hominid Evolution: Past, Present and Future. Alan R. Liss, New York, pp. 255–263.
Frost, S.R., 2001. Fossil Cercopithecidae of the Afar Depression, Ethiopia: Species Systematics and Comparison to the Turkana Basin (PhD dissertation). New York: City University of New York.
Frost, S.R., Marcus, L.F., Bookstein, F.L., Reddy, D.P., Delson, E., 2003. Cranial allometry, phylogeography, and systematics of large-bodied Papionins (Primates: Cercopithecinae) inferred from geometric morphometric analysis of landmark data. Anat. Rec. 275A, 1048–1072.
Gabounia, L., de Lumley, M.-A., Berillon, G., 2000. Morphologie et fonction du troisième métatarsien de Dmanissi, Gèorgie orientale. In: Lordkipanidze, D., Bar- Yosef, O., Otte, M. (Eds.), Early Humans at the Gates of Europe. University of Liege, Liege, pp. 29–41.
Gabounia, L., de Lumley, M.-A., Vekua, A., Lordkipanidze, D., de Lumley, H., 2002. Découverte d'un nouvel hominidé à Dmanissi (Transcaucasie, Géorgie). C.R. Pale. 1, 243–253.
Gillespie, R., 2002. Dating the first Australians. Radiocarbon 44, 455–472.
Gordon, A.D., Nevell, L., Wood, B., 2008. The *Homo floresiensis* cranium (LB1): size, scaling, and early *Homo* affinities. Proc. Natl. Acad. Sci. 105, 4650–4655.
Gower, J.C., 1975. Generalized procrustes analysis. Psychometrika 40, 33–51.
Groves, C.P., 2001. Primate Taxonomy. Smithsonian Institution Press, Washington, D.C.
Grün, R., Thorne, A., 1997. Dating the Ngandong humans. Science 276, 1575–1576.
Gunz, P., Harvati, K., 2007. The Neanderthal "chignon": variation, integration, and homology. J. Hum. Evol. 52, 262–274.
Harvati, K., 2001. The Neanderthal Problem: 3-D Geometric Morphometric Models of Cranial Shape Variation Within and Among Species (PhD dissertation). New York: City University of New York.
Harvati, K., 2003. The Neanderthal taxonomic position: models of intra-and interspecific craniofacial variation. J. Hum. Evol. 44, 107–132.
Harvati, K., Frost, S.R., McNulty, K.P., 2004. Neanderthal taxonomy reconsidered: implications of 3D primate models of intra-and interspecific differences. Proc. Natl. Acad. Sci. USA 101, 1147–1152.
Henneberg, M., Thorne, A., 2004. Flores may be pathological *Homo sapiens*. Before Farming 1, 2–4.
Hershkovitz, I., Kornreich, L., Laron, Z., 2007. Comparative skeletal features between *Homo floresiensis* and patients with primary growth hormone insensitivity (Laron Syndrome). Am. J. Phys. Anthropol. 134, 198–208.
How, R.A., Kitchener, D.J., 1997. Biogeography of Indonesian snakes. J. Biogeogr. 24, 725–735.
How, R.A., Schmitt, L.H., Maharadatunkamsi, 1996. Geographical variation in the genus *Dendrelaphis* (Serpentes: Colubridae) within the Banda Arc islands of Indonesia. J. Zool. Lond. 238, 351–363.
Howell, F.C., 1978. Hominidae. In: Maglio, V.J., Cooke, H.B.S. (Eds.), Evolution of African Mammals. Harvard University Press, Cambridge, pp. 154–248.
Howells, W.W., 1973. Cranial variation in man. Pap. Peabody Mus. Amer. Archaeol. and Ethnol. 67, 1–259.
Howells, W.W., 1980. *Homo erectus*—who, when and where: a survey. Yearb. Phys. Anthropol 23, 1–23.
Huffman, O.F., 2001. Geologic context and age of the Perning/Mojokerto *Homo erectus*, East Java. J. Hum. Evol. 40, 353–362.
Huffman, O.F., Shipman, P., Hertler, C., de Vos, J., Aziz, F., 2005. Historical evidence of the 1936 Mojokerto skull discovery, East Java. J. Hum. Evol. 48, 321–363.
Huffman, O.F., Zaim, Y., Kappelman, J., Ruez Jr., D.R., de Vos, J., Rizal, Y., Aziz, F., Hertler, C., 2006. Relocation of the 1936 Mojokerto skull discovery site near Perning, East Java. J. Hum. Evol. 50, 431–451.
Jacob, T., Indriati, E., Soejono, R.P., Hsü, K., Frayer, D.W., Eckhardt, R.B., Kuperavage, A.J., Thorne, A., Henneberg, M., 2006. Pygmoid Australomelanesian *Homo sapiens* skeletal remains from Liang Bua, Flores: population affinities and pathological abnormalities. Proc. Natl. Acad. Sci. USA 103, 13421–13426.
Jungers, W.L., Harcourt-Smith, W.E.H., Larson, S.G., Morwood, M.J., Djubiantono, T., 2008. Hobbit bipedalism: functional anatomy of the foot of *Homo floresiensis*. Am. J. Phys. Anthropol. 135 (S46), 127.
Kaifu, Y., Baba, H., Aziz, F., Indriati, E., Schrenk, F., Jacob, T., 2005. Taxonomic affinities and evolutionary history of the early Pleistocene hominids of Java: dentognathic evidence. Am. J. Phys. Anthropol. 128, 709–726. not cited in this version.
Kitchener, D.J., Suyanto, A., 1996. Intraspecific morphological variation among island populations of small mammals in southern Indonesia. In: Kitchener, D.J., Suyanto, A. (Eds.), In: Proceedings of the First International Conference on Eastern Indonesia-Australian Vertebrate Fauna. LIPI, Manado, Indonesia, pp. 7–13. not cited in this version.
Krantz, G.S., 1975. An explanation for the diastema of Javan erectus Skull IV. In: Tuttle, R.H. (Ed.), Paleoanthropology, Morphology and Paleoecology. Mouton, The Hague, pp. 361–372.
Lahr, M.M., Foley, R., 2004. Human evolution writ small. Nature 431, 1043–1044.
Lambeck, K., Chappell, J., 2001. Sea level change through the last glacial cycle. Science 292, 679–686.
Larick, R., Ciochon, R.L., Zaim, Y., Sudijono, Suminto, Rizal, Y., Aziz, F., Reagan, M., Heizler, M., 2001. Early Pleistocene $^{40}Ar/^{39}Ar$ ages for Bapang Formation hominins, Central Jawa, Indonesia. Proc. Natl. Acad. Sci. USA 98, 4866–4871.
Larson, S.G., Jungers, W.L., Morwood, M.J., Sutikna, T., Jatmiko, Saptomo, E.W., Rokus Awe Due, Djubiantono, T., 2007. *Homo floresiensis* and the evolution of the hominin shoulder. J. Hum. Evol. 53, 718–731.
Le Gros Clark, W.E., 1964. The Fossil Evidence for Human Evolution. University of Chicago Press, Chicago.
Leigh, S.R., Shah, N.F., Buchanan, L.S., 2003. Ontogeny and phylogeny in papionin primates. J. Hum. Evol. 45, 285–316.
Lordkipanidze, D., Jashashvili, T., Vekua, A., Ponce de León, M.S., Zollikofer, C.P.E., Rightmire, G.P., Pontzer, H., Ferring, R., Oms, O., Tappen, M., Bukhsianidze, M., Agusti, J., Kahlke, R., Kiladze, G., Martinez-Navarro, B., Mouskhelishvili, A., Nioradze, M., Rook, L., 2007. Postcranial evidence from early *Homo* from Dmanisi, Georgia. Nature 449, 305–310.
Lordkipanidze, D., Vekua, A., Ferring, R., Rightmire, G.P., Agusti, J., Kiladze, G., Mouskhelishvili, A., Nioradze, M.S., Ponce de León, M.S., Tappen, M., Zollikofer, C.P.E., 2005. The earliest toothless hominin skull. Nature 434, 717.
de Lumley, M.-A., Gabounia, L., Vekua, A., Lordkipanidze, D., 2006. Les restes humains du Pliocène final et du dèbut du Pléistocène inféfieur de Dmanissi, Géorgie (1991–2000). I - Les crânes, D 2280, D 2282, D 2700. L'Anthropologie 110, 1–110.
Mann, A., 1971. *Homo erectus*. In: Dolhinow, P., Sarich, V. (Eds.), Background for Man. Little, Brown, Boston, pp. 166–177.
Martin, R.D., MacLarnon, A.M., Phillips, J.L., Dussubieux, L., Williams, P.R., Dobyns, W.B., 2006a. Comment on "The brain of LB1, *Homo floresiensis*". Science 312, 999.
Martin, R.D., MacLarnon, A.M., Phillips, J.L., Dobyns, W.B., 2006b. Flores hominid: new species of microcephalic dwarf? Anat. Rec 288A, 1123–1145.
Mayr, E., 1944. Wallace's line in the light of recent zoogeographic studies. Q. Rev. Biol. 19, 1–14.
McNulty, K.P., 2003. Geometric Morphometric Analyses of Extant and Fossil Hominoid Craniofacial Morphology. Ph.D. Dissertation, City University of New York.
McNulty, K.P., Frost, S.R., Strait, D.S., 2006. Examining affinities of the Taung child by developmental simulation. J. Hum. Evol. 51, 274–296.
Miller, J.M.A., Albrecht, G.H., Gelvin, B.R., 2004. Craniometric variation in early *Homo* compared to modern gorillas: a population-thinking approach. In: Anapol, F., German, R.Z., Jablinski, N.G. (Eds.), Shaping Primate Evolution: Form, Function and Behavior. Cambridge University Press, Cambridge, pp. 66–98.
Mitteroecker, P., Gunz, P., Bernhard, M., Schaefer, K., Bookstein, F.L., 2004. Comparison of cranial ontogenetic trajectories among great apes and humans. J. Hum. Evol. 46, 679–698.
Morwood, M.J., Aziz, F., Van den Bergh, G.D., Sondaar, P.Y., De Vos, J., 1997. Stone artefacts from the 1994 excavation at Mata Menge, west central Flores, Indonesia. Aust. Archaeol 44, 26–34.
Morwood, M.J., Brown, P., Jatmiko, Sutikna, T., Saptomo, E.W., Westaway, K.E., Rokus Awe Due, Roberts, R.G., Maeda, T., Wasisto, S., Djubiantono, T., 2005. Further

evidence for small-bodied hominins from the Late Pleistocene of Flores, Indonesia. Nature 437, 1012–1017.
Morwood, M.J., O'Sullivan, P.B., Aziz, F., Raza, A., 1998. Fission-track ages of stone tools and fossils on the east Indonesian island of Flores. Nature 392, 173–176.
Morwood, M.J., O'Sullivan, P.B., Aziz, F., Raza, A., 1999. Archaeological and palaeontological research in central Flores, east Indonesia: results of fieldwork 1997–1998. Antiquity 73, 273–286.
Morwood, M.J., Soejono, R.P., Roberts, R.G., Sutikna, T., Turney, C.S.M., Westaway, K.E., Rink, W.J., Zhao, J-x., van den Bergh, G.D., Rokus Awe Due, Hobbs, D.R., Moore, M.W., Bird, M.I., Fifield, L.K., 2004. Archaeology and age of a new hominin from Flores in eastern Indonesia. Nature 431, 1087–1091.
Nevell, L., Gordon, A.D., Wood, B., 2007. *Homo floresiensis* and *Homo sapiens* size-adjusted cranial shape variation. Am. J. Phys. Anthropol. 132, 177–178 (Abstract).
Obendorf, P.J., Oxnard, C.E., Kefford, B.J., 2008. Are the small human-like fossils found on Flores human endemic cretins? Proc. Biol. Sci. 275, 1287–1296.
O'Higgins, P., 2000. The study of morphological variation in the hominid fossil record: biology, landmarks and geometry. J. Anat. 197, 103–120.
O'Higgins, P., Jones, N., 2006. Morphologika 2, v. 2.4. Hull York Medical School, York.
Richards, G.D., 2006. Genetic, physiologic and ecogeographic factors contributing to variation in *Homo sapiens*: *Homo floresiensis* reconsidered. J. Evol. Biol. 19, 1744–1767.
Rightmire, G.P., 1990. The Evolution of *Homo erectus*: Comparative Anatomical Studies of an Extinct Human Species. Cambridge University Press, Cambridge.
Rightmire, G.P., Lordkipanidze, D., Vekua, A., 2006. Anatomical descriptions, comparative studies and evolutionary significance of the hominin skulls from Dmanisi, Republic of Georgia. J. Hum. Evol. 50, 115–141.
Robinson, J.T., 1953. *Telanthropus* and its phylogenetic significance. Am. J. Phys. Anthropol. 11, 445–501. not cited in this version.
Rohlf, F.J., Marcus, L.F., 1993. A revolution in morphometrics. Trends Ecol. Evol. 8, 129–132.
Rohlf, F.J., Slice, D., 1990. Extensions of the Procrustes method for the optimal superimposition of landmarks. Sys. Zool. 39, 40–59.
Ruff, C.B., Walker, A., 1993. Body size and body shape. In: Walker, A., Leakey, R. (Eds.), The Nariokotome *Homo erectus* Skeleton. Harvard University Press, Cambridge, pp. 234–265.
Sciulli, P.W., Doyle, W.J., Kelley, C., Siegel, P., Siegel, M.I., 1979. The interaction of stressors in the induction of increased levels of fluctuating asymmetry in the laboratory rat. Am. J. Phys. Anthropol. 50, 279–284.
Shea, B.T., Bailey, R.C., 1996. Allometry and adaptation of body proportions and stature in African pygmies. Am. J. Phys. Anthropol. 100, 311–340.
Siegel, M.I., Doyle, W.J., Kelley, C., 1977. Heat stress, fluctuating asymmetry and prenatal selection in the laboratory rat. Am. J. Phys. Anthropol. 46, 121–126.
Slice, D.E., 1998. Morpheus et al. Software for Morphometric Research. Department of Ecology, State University of New York, Stony Brook, New York.
Slice, D.E., 2001. Landmark coordinates aligned by Procrustes analysis do not lie in Kendall's shape space. Syst. Biol. 50, 141–149.
Sondaar, P.Y., 1984. Faunal evolution and the mammalian biostratigraphy of Java. Cour. Forsch.-Inst. Senckenberg 69, 219–235.
Sondaar, P.Y., 1987. Pleistocene man and extinctions of island endemics. Mem. Soc. Geol. Fr. 150, 159–165.
Sondaar, P.Y., Van den Bergh, G.D., Mubroto, B., Aziz, F., de Vos, J., Batu, U.L., 1994. Middle Pleistocene faunal turnover and colonization of Flores (Indonesia) by *Homo erectus*. Comptes rendus Ac. Sci. F. Sér. II 319, 1255–1262.
Swaddle, J.P., Witter, M.S., 1994. Food, feathers and fluctuating asymmetry. Proc. R. Soc. Lond. B Biol Sci 255, 147–152.
Swisher III, C.C., 1997. A revised geochronology for the Plio-Pleistocene hominid bearing strata from Sangiran, Java. J. Hum. Evol. 32, A23.
Swisher III, C.C., Curtis, G.H., Jacob, T., Getty, A.G., Suprijo, A., Widiasmoro, 1994. The age of the earliest hominids in Java, Indonesia. Science 263, 1118–1121.
Swisher III, C.C., Rink, W.J., Antón, S.C., Schwarcz, H.P., Curtis, G.H., Suprijo, A., Widiasmoro, 1996. Latest *Homo erectus* of Java: potential contemporaneity with *Homo sapiens*. Science 274, 1870–1874.
Tattersall, I., Sawyer, G.J., 1996. The skull of "*Sinanthropus*" from Zhoukoudian, China: a new reconstruction. J. Hum. Evol. 31, 311–314.
Tobias, P.V., von Koenigswald, G.H.R., 1964. A comparison between the Olduvai hominines and those of Java and some implications for hominid phylogeny. Curr. Anthropol. 6, 427–431.
Tocheri, M.W., Orr, C.M., Larson, S.G., Sutikna, T., Jatmiko, Saptomo, E.W., Rokus Awe Due, Djubiantono, T., Morwood, M.J., Jungers, W.L., 2007. The primitive wrist of *Homo floresiensis* and its implications for hominin evolution. Science 317, 1743–1745.
Turner, A., Chamberlain, A., 1989. Speciation, morphological change and the status of African *Homo erectus*. J. Hum. Evol. 18, 115–130.
Van den Bergh, G.D., de Vos, J., Sondaar, P.Y., 2001. The Late Quaternary palaeogeography of mammal evolution in the Indonesian Archipelago. Palaeogeogr., Palaeoclimatol., Palaeoecol 171, 385–408.
Van den Bergh, G.D., Meijer, H.J.M., Rokhus Due Awe, Morwood, M.J., Szabó, K., Van den Hoek Ostende, L.W., Sutikna, T., Saptomo, E.W., Piper, P.J., Dobney, K.M., 2009. The Liang Bua faunal remains: a 95 k.yr. sequence from Flores, East Indonesia. J. Hum. Evol. 57 (5), 527–537.
Vekua, A., Lordkipanidze, D., Rightmire, G.P., Agusti, J., Ferring, R., Maisuradze, G., Mouskhelishvili, A., Nioradze, M., De Leon, M.P., Tappen, M., Tvalchrelidze, M., Zollikofer, C., 2002. A new skull of early *Homo* from Dmanisi, Georgia. Science 297, 85–89.
Voris, H.K., 2000. Maps of Pleistocene sea levels in Southeast Asia: shorelines, river systems and time durations. J. Biogeogr. 27, 1153–1167.
Wang, Q., Tobias, P.V., 2001. An old species and a new frontier: some thoughts on the taxonomy of *Homo erectus*. Przeglad Antropologiczny-Anthropol. Rev. 64, 9–20.
Weber, J., Czarnetzki, A., Pusch, C.M., 2005. Comment on "The brain of LB1, *Homo floresiensis*". Science 310 236b.
Weidenreich, F., 1943. The skull of *Sinanthropus pekinensis*: a comparative study on a primitive hominid skull. Palaeontologica Sinica D10, 1–485.
Weidenreich, F., 1951. Morphology of Solo Man. Anthropol. Pap. Am. Mus. Nat. Hist. 43, 222–288.
Westaway, M., Jacob, T., Aziz, F., Otsuka, H., Baba, H., 2003. Faunal taphonomy and biostratigraphy at Ngandong, Java, Indonesia and its implications for the late survival of *Homo erectus*. Am. J. Phys. Anthropol. 120 (S36), 222–223.
White, T.D., 1995. African omnivores: global climatic change and Plio-Pleistocene hominids and suids. In: Vrba, E.S., Denton, G.H., Partridge, T.C., Burckle, L.H. (Eds.), Paleoclimate and Evolution, with Emphasis on Human Origins. Yale University Press, New Haven, pp. 369–385.
White, T.D., Folkens, P.A., 2000. Human Osteology, second ed. Academic Press, New York.
Wood, B.A., 1984. The origin of *Homo erectus*. Cour. Forsch.-Inst. Senckenberg 69, 111.
Wood, B.A., 1991. Koobi Fora Research Project: Hominid Cranial Remains. Oxford University Press, New York.